II.9. DETRA

1. MODEL DESCRIPTION AND EVALUATION OF MODEL PERFORMANCE

V. SUOLANEN
VTT Energy, Nuclear Energy,
Helsinki, Finland

2 MODEL DESCRIPTION

2.1 Name of model, model developer, model user

The numerical calculations have been performed employing the computer code DETRA [3] (*Doses via Environmental Transfer of Radionuclides*). The DETRA code has been originally developed by Dr. Ilkka Savolainen and Dr. Riitta Korhonen from VTT. The present user of the code is Vesa Suolanen.

The DETRA code employs a dynamic compartment approach. Except for the fish model [4], the conceptual models i.e. the compartment models to simulate the transfer of cesium via different pathways of Test Scenario S have been created by the user. Some dose calculations were performed by additional analytical equations.

2.2 Important model characteristics

2.2.1 Intended purpose of the model in radiation assessment

The computer code DETRA is a generic tool for environmental transfer analyses of radioactive or stable substances. The code has been applied for various purposes, mainly problems related to the biospheric transfer of radionuclides both in safety analyses of disposal of nuclear wastes and in consideration of foodchain exposure pathways in the analyses of off-site consequences of reactor accidents. For each specific application an individually tailored conceptual model can be developed. The biospheric transfer analyses performed by the code are typically carried out for terrestrial, aquatic and food chain applications.

2.2.2 Intended accuracy of the model prediction

The intended accuracy of the model predictions depends on the specific application, but in the type of analyses discussed in this report the intended accuracy is roughly within a factor of about 10, based on the estimation of uncertainty related to the conceptual models and to the input parameters.

2.2.3 Method used for deriving uncertainty estimates

The uncertainty estimates were derived based on simplified Monte Carlo type analyses for the most important parameters. Basically the model at present employs a deterministic approach.

2.2.4 Past experiences using this model

The total set of the conceptual sub-models applied in the context of this exercise was used for the first time. Past experiences of the sub-models have, however, shown in many cases harmonic temporal behaviour with the observed values available. Considerable experience has been gained in modelling pasture and aquatic environment while the metabolic models of domestic animals have been created recently.

1 TEST SCENARIO S

The Multiple Pathways Assessment (MPA) Working Group aims to test models that predict doses to actual population groups living in contaminated environments. Therefore, the models may have to be capable of predicting doses arising from pathways related to different environments. Ingestion pathways related to terrestrial and aquatic environments, inhalation of contaminated air either directly or after resuspension, as well as external exposure from contaminated surfaces or from the radioactive discharge plume are included in the model predictions.

After the Chernobyl accident, suitable data sets for testing these models exist in several countries. The observed data provide the modellers an opportunity for testing their ability to predict the temporal behaviour of cesium concentrations in foodstuffs and in the bodies of human populations. The exercises in the MPA working group are being carried out as so-called 'blind-tests', i.e. the modellers receive a scenario description and are provided with the observation data only after their predictions have been submitted to the Secretariat.

Test Scenario S uses data from Finland [1]. The deposition area considered in Test Scenario S is presented in Fig. 1. The area of S includes fully the area of the highest deposition intensity measured in Finland after the Chernobyl accident. Fig. 2 presents the relative position of population areas (POP1, POP2, ..., POP9) and air sampling stations (AIR1, AIR2) given in the scenario description [1]. Furthermore, the relative positions of agricultural areas (AGR1, AGR2, ... , AGR17) and fish catchment areas (FISH1, FISH2, ..., FISH6) are presented in Figs. 3 and 4 [1].

The modelling tasks, predictions, and comparison of observed data vs predictions of Test Scenario S are presented in the following text of this report.

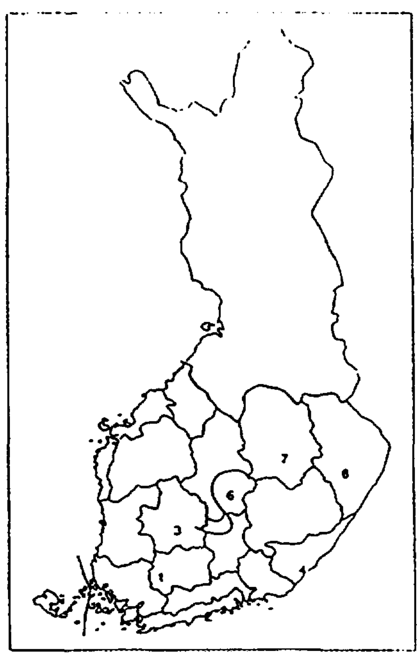

Fig. 1. Deposition area of Test Scenario S.

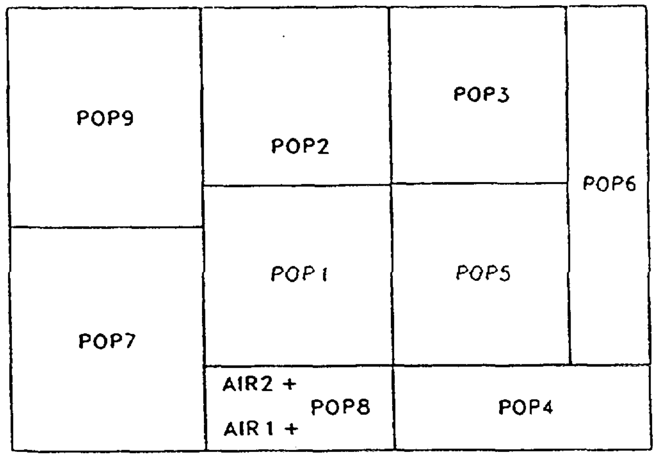

Fig. 2. Relative position of population areas (POP) and air sampling stations (AIR) [1].

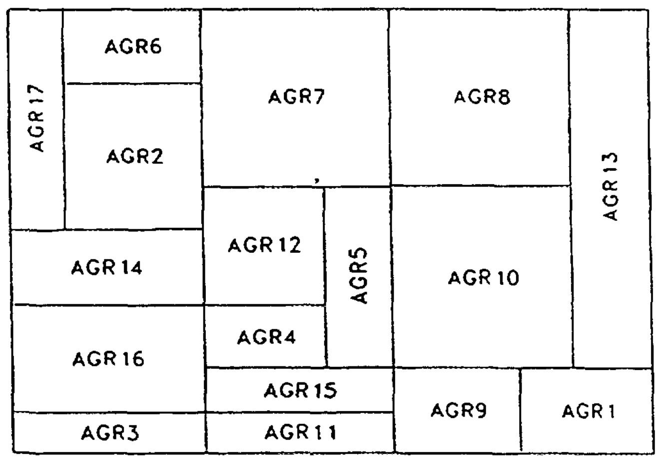

Fig. 3. Relative position of agricultural areas (AGR) [1].

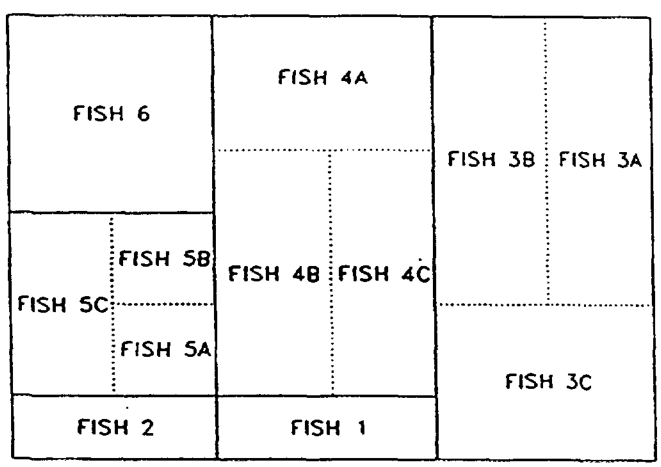

Fig. 4. Relative position of fish catchment areas (FISH) [1].

2.4 Model structure

Fig. 5. presents the structure of the compartment model used for pasture, grain and related pathways. The lines between each compartment describe the transfer of radionuclides from one compartment to another. A precondition for a reliable prediction of the contamination of milk, beef and pork is a successful modelling of the contamination of pasture and grain products. Simplified metabolic models for cows and pigs are used to estimate the accumulation of cesium in organisms of those animals.

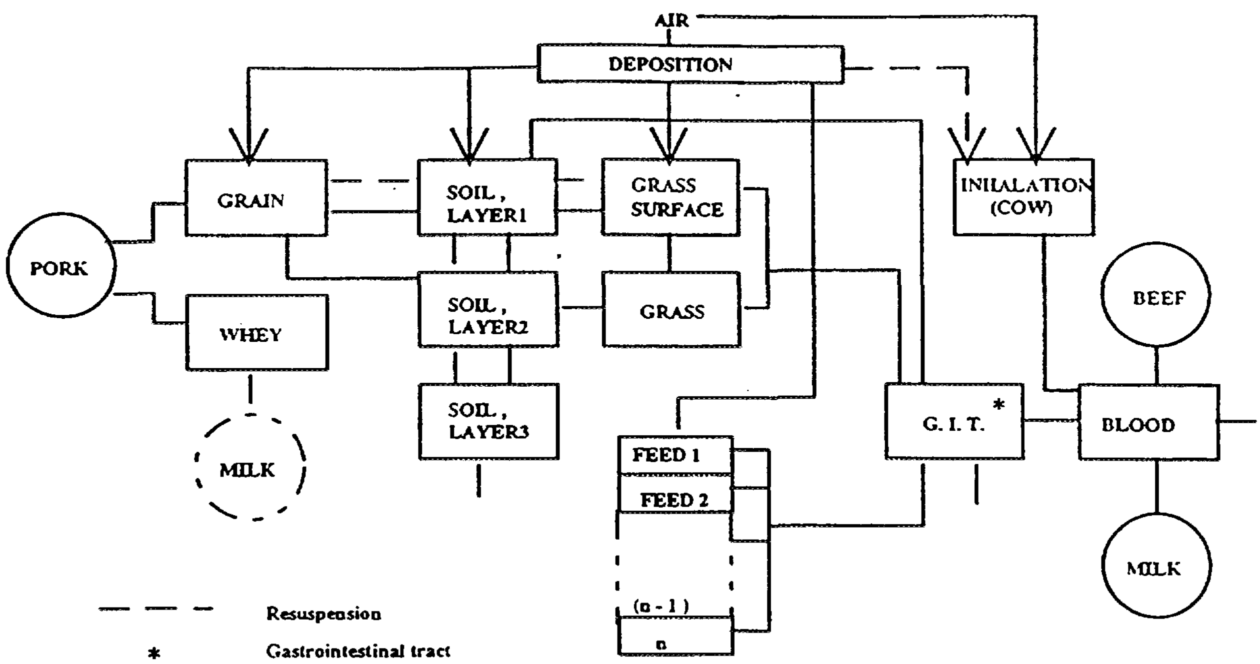

Fig. 5. The compartment model used for modelling pasture and related pathways.

Based on the description of scenario S, the beef cattle do not usually graze. Therefore, the consumption of soil particles of pasture was not considered in case of beef cattle. Additionally, the feed consumption rate for beef cattle is assumed to be one third of that for milk cattle [1].

The feed for pigs is assumed to consist mainly of mixed grain and a minor fraction (0.05) of the byproduct of milk, whey. The specific activity of cesium nuclides in whey is, however, higher by a factor of about 9.5 than for milk [5]. The activity inflow to pig organism might therefore be even higher via the consumption of contaminated whey than via the consumption of contaminated mixed grain.

Many uncertainty factors affect concentrations in animal products in the long term, such as contaminated soil particles which are sorbed on feed, changes in the solubility of elements, various agricultural practices, etc. The effect of these factors can approximately be considered e.g. with indirect methods such as assuming an additional, gradually decreasing fraction of contaminated material in the feed system of animals for some years after deposition.

The model used is based on sequential modelling approach by accounting multiple season sequences after deposition. The calculation procedure is based on realistic agricultural practices, i.e. modelling systematically the sequences of grazing periods and housed periods. The selective concentration values at the end of each grazing period are used as initial concentration values for the further calculation of the housed period and vice versa. According to the scenario description, the grazing period was assumed to start on the 10th of May and end on the 20th of September when the housed period starts.

2.5 Descriptions of procedures, equations and parameters used in different components of the model

2.5.1 Total deposition

The total deposition was calculated based on the measured deposition values of the sub-areas of Scenario S which were given in the scenario description [1]. By using the given deposition values and surface areas of the sub-areas, the mean total deposition value for the whole area of S is obtained as follows:

$$\bar{d}_S = \frac{1}{A_S} \cdot \sum d_i \cdot A_i$$

where

$\bar{d}_S$	is the mean total deposition over the area S, [Bq/m^2]
d_i	is the mean deposition of sub-area i, [Bq/m^2]
A_S	is the area of S, [m^2]
A_i	is the area of i, [m^2].

According to the scenario description, there were only a few measurement stations for collecting data for air concentrations. Because the area S is relatively large, it was decided to use the measured deposition values which are likely to give a more comprehensive and reliable picture of the deposition profile for the area S than an approach based on the use of air concentration. The calculated mean deposition value, based on measured values of sub-areas of area S, was assumed to be realistic for the purpose of further predictions of Scenario S. Reliable deposition values were also regarded as important considering prediction of the ingestion doses which were one of the main tasks of Scenario S. As a result, the mean deposition value, integrated over the whole area of Scenario S, was estimated to be 19.3 kBq/m^2.

The presented predicted concentration values of foodstuffs of Scenario S are weighted by deposition and by production values.

2.5.2 Foodstuffs contributing to total diet

2.5.2.1 Milk

The conceptual model employed is condensed in Fig. 5 above. The parameters and data are presented in Table I. Airborne ^{137}Cs was assumed to be deposited on grass, soil (and also on other crops such as grain, etc.). The time of the year in which the deposition of the Chernobyl release in the area S took place was late spring, end of April. At that time of the year and considering the milk model it was assumed that a fraction of 30 per cent of the deposited material was intercepted on the grass surface [6] and the rest of the material was assumed to have been deposited on soil surface. The interception factor between grass and deposited nuclides is directly proportional to the grass intensity on pasture [kg_{grass}/m^2], i.e. generally the leaf area of crops. The effective half-life of cesium on grass surface was assumed to be 25 days [7]. The loss rate of cesium from grass surface is affected by the intensities of rain and wind.

General method for prediction of the contamination level on the surface of grass or other leafy vegetation is given by:

$$A_{s,j}(t) = A_{s,j}(t_o) \cdot e^{-(\lambda_w + \lambda) \cdot t}$$

$$\lambda_w = \frac{ln2}{T_{½,w}}$$

$$\lambda = \frac{ln2}{T_{½}}$$

where

$A_{s,j}(t_o)$	is the initial surface activity on crop j, [Bq/m^2]
$A_{s,j}(t)$	is the temporal surface activity on crop j, [Bq/m^2]
λ_w	is the weathering loss-rate, [1/d]
λ	is the radioactive decay rate, [1/d]
$T_{1/2,w}$	is the weathering half-life, [d]
$T_{1/2}$	is the radioactive half-life, [d].

The model used accounts for the foliar uptake, but it was assumed to have only a minor effect when considering the transfer of cesium in the pasture system. The root uptake becomes relatively more important in the longterm. The resuspension of contaminated soil particles and their deposition on grass are modelled as well (see Fig. 5), although resuspension has in general only a minor effect on grass and milk contamination levels. In the case of Scenario S, the main contribution to the contamination of milk comes, however, from the effects of direct deposition.

The modelling approach of the milk model used is based on multiple season sequences. During the calculation, the grazing period and the housed period of cows are assumed to alternate in constant periods. Therefore, at the beginning of each calculation sequence, initialization of the concentrations in each relevant compartment is performed in the model.

The grazing period was assumed to start on 10th May and to end on 20th September, when the housed period of cows correspondingly starts [1]. Additionally, a grazing restriction up to the end of May was applied at the beginning of the calculation of Test Scenario S. Because the deposition occured at the end of April there was a period of one month during which the contamination level of grass decreased from the maximum value. By the time the cows were allowed to go on the pasture contamination level had therefore passed the maximum value. The real temporal behaviour of the contamination level of pasture was used in the calculation.

The assumed harvesting times of hay were 15th June, 15th July and the 15th of August, when the feed for the housed period was gathered. It was also assumed that for each harvesting time the yield is equal. The mean concentration value of feed can then be estimated based on the contamination levels of those three harvests.

In the longterm, many uncertainty factors such as contaminated soil in feed, changes in the solubility of elements, and matters related to agricultural practices affect the contamination level of milk and other domestic animal products. In order to account for these uncertainty factors and to apply a conservative modelling approach, it was assumed that the loss of contaminated material from the considered system will be delayed to some extent. Fig. 6 presents the assumed decrease in the amount of originally contaminated material in the feed of cows during the housed period after the deposition. The values employed for the fraction of contaminated material in feed in the years following the accident are based on a qualitative judgement and not on direct empirical observations.

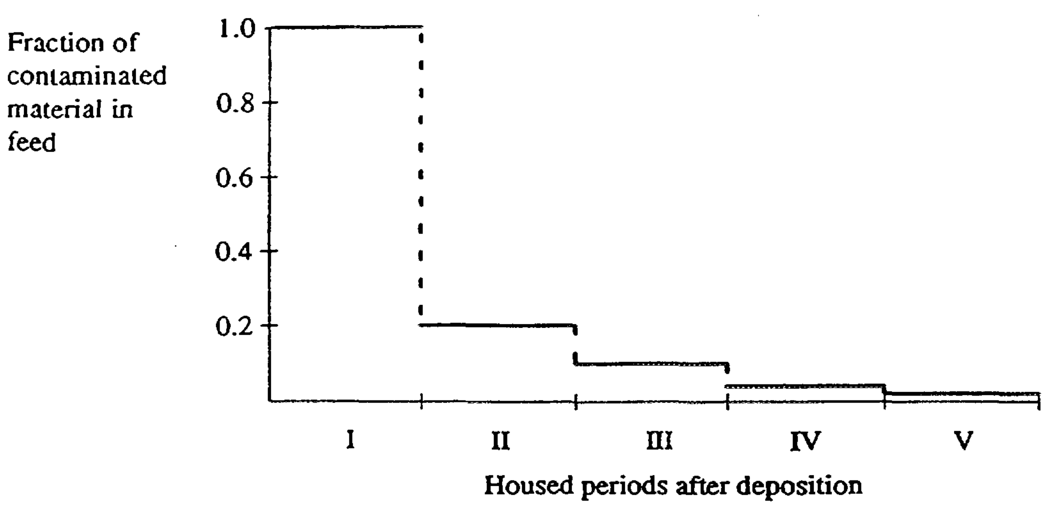

Fig. 6. The assumed amount of originally contaminated material in feed of cows during the housed periods after the deposition.

Besides being radiologically a very important foodstuff in itself, milk contributes to contamination levels in other foodstuffs such as pork. This is due to the fact that whey, a byproduct of milk, is used as feed for pigs. This question will be discussed in more detail in the context of pork. Additionally, the temporal behaviour of the contamination of beef is qualitatively closely related to the contamination of milk. The essential differences between milk and beef consist of different infiltration factors and metabolic time constants related to those foodstuffs.

Table I Data used in the pasture and milk models.

	Reference[1)]	General data of the model	Data for ^{137}Cs nuclide
PASTURE MODEL			
- grass intensity on pasture, [$kg_{d.w.}/m^2$]	[8]	0.45	
- grass interception factor for deposition	[6]		0.30
- initial fraction of soil sorbed on the grass surface[2)], [per cent of dry weight of grass]	[9]	4 ($T_{1/2}$ = 1 a)	
- radioactive half-life of nuclide, [a]			30
- effective half-life of cesium on grass surface, [d]	[7]		25
- soil to grass concentration factor, [$Bq/kg_{f.w.}$]/[Bq/kg_{soil}]	[10]		$2 \cdot 10^{-2}$
- absorption factor from grass surface into grass, [d^{-1}]	[11]		$2 \cdot 10^{-3}$
- soil layer[3)] 1: [cm]		0 -> 1	
- soil layer[3)] 2: [cm]		1 -> 5	
- soil layer[3)] 3: [cm]		5 -> 10	
- density of soil[3)], [kg/m^3_{soil}]		1650	
· water, [kg_w/m^3_{soil}]		300	
· solid matter, [kg_s/m^3_{soil}]		1350	
- distribution coefficient K_d, [liter/kg]	[12]		$1 \cdot 10^3$
- average rain intensity, [mm/d]	[13]	1.8	
- evaporation, [per cent of rain intensity]	[13]	45	
HOUSED PERIOD MODEL			
- assumed harvesting times in feed production:		15th June 15th July 15th August	
MILK CATTLE DATA			
- grass consumed by cow, [$kg_{f.w.}/d$]	[1]	50	
- soil consumed by cow during grazing, [kg_s/d]	[9]	2	
- average milk production of cow, [liter/cow/year]	[1]	4900	

1) Reference which is used directly or from which the data used in this study is derived.
2) The half-life for fraction of soil contamination on grass surface is assumed to be one year [14]. The used value for half-life is based on observed temporal behaviour of resuspension after deposition in the Nordic environment.
3) The data used is based on previous experience of environmental modelling and on review of literature.

2.5.2.2 Beef

The calculation method applied to predict the activity content in beef is presented above in Fig. 5. The additional data used are presented in Table II, other necessary data used to calculate the contamination level of beef were presented earlier in Table I. The calculation method for beef is very similar to the calculation method for the milk component. The reason for that is the similarity of the metabolism of the animal in the two cases. There are significant differences, however, in the metabolic infiltration factors and in the time constants needed to reach the steady state between the source term (i.e. the activity intake) and the contamination of the considered foodstuff. The time constant related to the contamination of beef is much larger than the time constant for milk. The biological half-life used for cesium in beef is 40 days [15]. Qualitatively the temporal behaviour of concentrations of cesium in beef and milk is of similar form, but the concentration curve of beef has a smoother tendency than the concentration curve of milk. The reasons for this were discussed above.

The consumption rate for feed beef cattle is lower than that for cows, because of the lower requirements of nutriments for beef cattle. The mean consumption rate used for grass for beef cattle is 17 $kg_{f.w.}/d$.

Table II *Data used in the beef model.*

	Reference[1)]	General data of the model	Data for ^{137}Cs nuclide
BEEF CATTLE DATA			
- grass eaten by beef cattle, [$kg_{f.w.}/d$]	[1]	17	
- biological half-life $T_{1/2b}$ in beef, [d]	[15]		40

1) Reference which is used directly or from which the data used in this study is derived.

2.5.2.3 Pork

The calculation method applied to predict the activity concentration in pork is presented above in Fig. 5. Some cereals data related to the pork model are presented in Table VIII, the other data of the pork model are presented in Table III.

The pig feed consists mainly of mixed grain feed [1], about 90 per cent, and the rest is assumed to be supplementary feed such as whey. Because the cesium activity concentration in dried whey is about 9.5 times higher than cesium concentration in dried milk [5], whey forms a very significant activity flux into the pig organism. Occasionally, activity flux via whey might be even higher than via intake of grain feeds.

A prerequisite for a successful prediction of the contamination level in pork is a sufficient accuracy of predictions of the contamination levels of grain and milk products which are used as pig feed. The modelling approach of grain is to a large extent of the same type as in the case of grass, although the interception properties and the derived interception factors of grass and grain differ.

The biological half-life of cesium in pork is assumed to be 18 days [15].

Table III Data used in the pork model[1)].

	Reference[2)]	General data of the model	Data for ^{137}Cs nuclide
DATA RELATED TO PIGS			
- mixed grain feed eaten by pigs, [kg/d]	[5]	1.5	
- whey eaten by pigs, [kg/d]	[5]	0.15	
- ingestion transfer factor, [d/kg]	[15]		$2.6 \cdot 10^{-1}$
- biological half-life $T_{1/2b}$ in pork, [d]	[15]		18

1) See also Table VIII, the cereals model.
2) Reference which is used directly or from which the data used in this study is derived.

2.5.2.4 Game

The activity concentration in game meat is proportional to the activity concentration in the forest soil. The concentration of cesium in game has been estimated by applying the following equations:

For summer and autumn ($t_o \le t \le t_1$):

$$C_{game}(t) = C_s(t) \cdot c_v \cdot J_v \cdot f_g \cdot (1 - e^{-\frac{\ln 2}{T_{1/2,b}} \cdot (t - t_o)})$$

For winter ($t_1 < t < t_o$):

$$C_{game}(t) = C_{game}(t_1) \cdot e^{-\frac{\ln 2}{T_{1/2,b}} \cdot (t - t_1)}$$

where

C_{game}	is the concentration of cesium in game meat, [Bq/kg]
C_s	is the concentration in forest soil, [Bq/kg$_{f.w.}$]
c_v	is the forest soil to forest vegetation concentration factor
J_v	is the consumption rate of vegetation by the game animal, [kg/d]
f_g	is the ingestion transfer factor of the game animal, [d/kg]
$T_{1/2,b}$	is the biological half-life of cesium in game, [d]
t_o	is the time point of 1 May
t_1	is the time point of 31 December.

According to analyses performed by the soil model, the cesium activity concentration in forest soil decreases slowly. In the case of ^{137}Cs the decrease rate of the activity level in forest soil is about five per cent per year. Thus the decrease of the activity concentration in game meat will also be relatively slow. The diet of game is different according to the season. During the winter the diet of game includes probably less contaminated material which tends to decrease the cesium concentration in game.

The data used in the game model are presented in Table IV.

Table IV *The data used in the game model.*

	General data of the model	Data for ^{137}Cs nuclide and consumption rates:	
		Big game	*Small game*
GAME			
- ingestion transfer factor[1], [d/kg]		$4 \cdot 10^{-2}$	$9 \cdot 10^{-2}$
- biological half-life[1], [d]		40	30
- eff. soil to forest vegetation transfer factor[2], $[Bq/kg_{f.w.}]/[Bq/kg_{forest\ soil}]$	0.5		
- consumption rates of vegetation[1], $[kg_{f.w.}/d]$		9	2

1) See explanation 3) under Table I.
2) Includes all kinds of vegetation, such the contaminated organic material in the top layer of forest soil, mushrooms, etc.

2.5.2.5 Wild berries

The activity concentration in wild berries, such as blueberry and lingonberry, is proportional to the activity concentration in forest soil. Therefore, the prediction of the cesium concentrations in wild berries was based on dynamic calculation of the surface activity concentration in forest soil (up to 1.5 centimeters depth in soil) after the deposition. Subsequently, the concentration factor method was applied to calculate the concentrations in berries at harvesting times based on forest soil concentrations. The activity concentration in soil was calculated with a compartment model, as shown above in Fig. 5, to simulate the vertical migration of cesium nuclides in the forest soil. The data used are presented in Table V. The soil to berries transfer factor represents a mean value applied for various types of berries.

Table V *Data used in the wild berries model.*

	General data of the model	Data for ^{137}Cs nuclide
WILD BERRIES		
- soil to berries transfer factor[1], $[Bq/kg_{f.w.,berry}]/[Bq/kg_{forest\ soil}]$		0.1
- harvesting time	31st August	

1) See explanation 3) under Table I.

2.5.2.6 Mushrooms

As in the case of wild berries, the activity concentration in mushrooms is also proportional to the activity concentration in the forest soil. The mushrooms grow out of a so-called mycelium which spreads out widely in the soil. The mycelium increases the transfer of radionuclides from the soil to the mushrooms, because the contact surface area for infiltration is remarkably larger. Also, in the case of Scenario S, the mushrooms had to penetrate the contaminated soil surface and thereby interact with soil particles. It is easy to see that the contaminated soil particles will, to some extent, be sorbed on the surface of the mushrooms. Considering the circumstances mentioned above, it was concluded to increase the concentration effect and concentration factors compared to wild berries. Otherwise, the modelling approach for mushrooms is of the same type as for wild berries. The data used are presented in Table VI.

Table VI *Data used in the mushrooms model.*

	General data of the model	Data for ^{137}Cs nuclide
MUSHROOMS		
- soil to mushrooms transfer factor[1)], $[Bq/kg_{f.w.,mushroom}]/[Bq/kg_{forest\ soil}]$		0.5
- harvesting time	15th October	

1) See explanation 3) under Table I and the text above.

2.5.2.7 Leafy vegetables

According to the information given in Scenario S description, most of the leafy vegetables are grown in greenhouses. Therefore, the average deposition value of area S has to be reduced in order to obtain a realistic value of deposition on leafy vegetables in greenhouses. The reduction of the activity content of air in greenhouses is caused by infiltration from the atmosphere into the greenhouses. The phenomena which accounted for the contamination of leafy vegetables were deposition and resuspension during the first summer and autumn seasons, and only resuspension thereafter.

After the assumed deposition on leafy vegetables, the loss of radionuclides from the surface of leafy vegetables is traditionally calculated by applying a given half-life. The data used for leafy vegetables are presented in Table VII.

2.5.2.8 Cereals

The conceptual calculation method used is presented in Fig. 5 above. The essential data in the prediction of the contamination level of cereals is the initial interception factor between cereals and the deposited radionuclides on the one hand, and the effective loss rate of nuclides from the surface of cereals in the later phase on the other. Table VIII presents the used data.

After ploughing, the soil contamination level is recalculated, based on the concentration profile of the soil before ploughing.

Table VII Data used in the leafy vegetables model.

	Reference[1)]	General data of the model	Data for ^{137}Cs nuclide
LEAFY VEGETABLES			
- yield, [$kg_{f.w.}/m^2$]	[8]	1	
- soil contamination on surface of leafy vegetables, [per cent of dry weight of vegetable]	[9]	0.01	
- effective half-life of cesium on surface of leafy vegetable, [d]	[7]		30
- infiltration factor for greenhouses[2)]			0.05
- interception factor[3)]			0.3

1) Reference which is used directly or from which the data used in this study is derived.

2) Educated guess based on the sealing properties of greenhouses.

3) Effective interception factor applied in the case of greenhouses is: interception factor · infiltration factor = 0.3 · 0.05 = 0.02

Table VIII The data used in the cereals model.

	Reference[1)]	General data of the model	Data for ^{137}Cs nuclide
CEREALS			
- yield, [$kg_{d.w.}/m^2$]	[8]	0.4	
- interception factor (grain):	[16]		0.05 (rye[2)]) 0.005 (others)
- initial fraction of soil on surface of cereals, [per cent of dry weight of grain]	[9]	0.01	
- effective weathering half-life, [d]	[7]		32
- harvesting time:			15th August
- soil to cereals transfer factor, [$Bq/kg_{f.w.}$]/[Bq/kg_{soil}]	[10]		$1 \cdot 10^{-2}$

1) Reference which is used directly or from which the data used in this study is derived.

2) The interception factor of rye accounts for the additional contamination effect of soil particles which were assumed to be sorbed on winter rye when rye penetrated the contaminated soil layer in the spring. Cesium was assumed to be transfered into cereals by translocation and by root uptake.

2.5.2.9 Fish

The method of predicting the contamination of freshwater fish in area S is based on the utilization of three selected lake size classes, three selected environmental sorption classes and on the dynamic fish model for non-predatory, intermediate and predatory fish types. The compartment structure of the fish model is presented in Fig. 7 below. Detailed information on this type of a dynamic fish model is given in ref. [4].

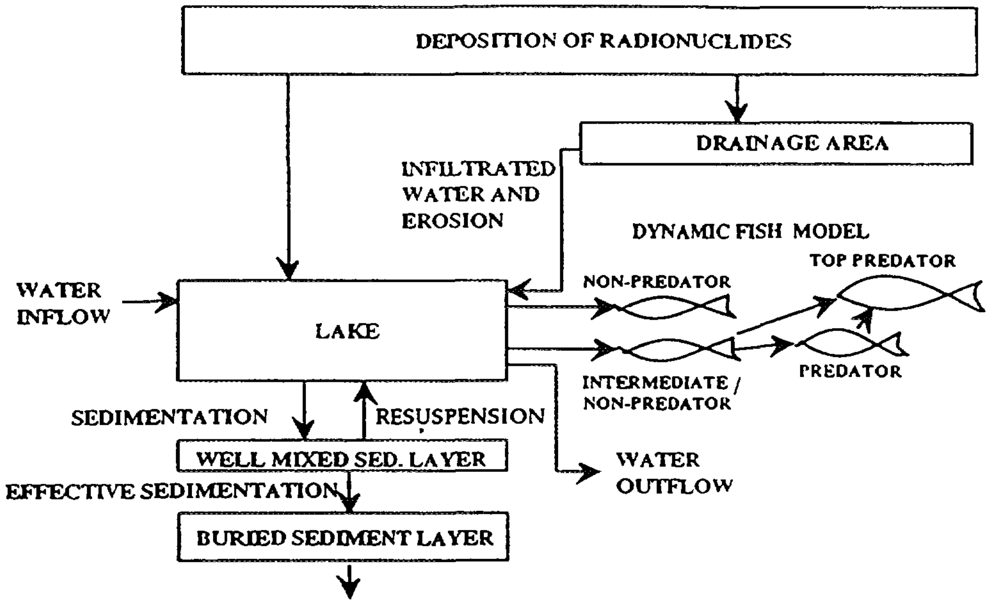

Fig. 7. The compartment model used for fish and related pathways.

The characteristics of different selected sizes of lakes are presented in Table IX. The selection of lake size classes is based on information given in the scenario description [1]. The dilution property of a lake, i.e. lake volume multiplied by the water exchange rate, is an essential factor when predicting not only the contamination of lake water but also the contamination of various fish types. Additionally, the sorption properties related to the considered aquatic environment affect the concentration of radionuclides in fish.

The deposition area of S was divided into six fishing areas which have different areal occurrence probabilities of lake sizes. The occurrence probabilities of different selected lake sizes and mean areal deposition values in different fishing areas are presented in Table X. The selection of occurrence probabilities of lakes sizes is based on a rough investigation of areal maps available of the area S.

In the first phase of the calculation procedure, the mean concentration values of different fish types (non-predatory, intermediate and predatory) of sub-areas (FISH1, FISH2, ..., FISH6) [1] were determinated as a function of time. In the second phase, the results of the sub-areas were integrated to obtain the mean fish concentrations of the whole area S.

Table IX *The characteristics of the used lake types.*

Lake surface area,	Effective drainage area,	Mean depth of lake,	Suspended sediment load of lake and sedim. rate	Water exchange rate,	Sorption distribution coefficient, $[Bq/kg_s]/[Bq/liter_w]$		
$[km^2]$	$[km^2]$	[m]	$[kg_s/m^3]$ or $(kg_s/m^2/a)$	[1/a]	class 1[1)]	class 2[2)]	class 3[3)]
1	2	2.5	$1.5 \cdot 10^{-3}$ (0.5)	2	$1.1 \cdot 10^3$	$1 \cdot 10^3$	$9 \cdot 10^2$
100	300	5	$1 \cdot 10^{-3}$ (0.2)	1	$1.1 \cdot 10^3$	$1 \cdot 10^3$	$9 \cdot 10^2$
1000	1000	7	$1 \cdot 10^{-3}$ (0.2)	1	$1.1 \cdot 10^3$	$1 \cdot 10^3$	$9 \cdot 10^2$

1) Fishing areas [1]: FISH1, FISH2, FISH5, FISH6
2) Fishing areas [1]: FISH4
3) Fishing areas [1]: FISH3

Table X *The occurrence probabilities of different lake sizes of area S and the mean deposition rates in fishing areas FISH1 to FISH6.*

Fishing area	Occurrence probabilities			Mean deposition of ^{137}Cs [1], $[kBq/m^2]$
	Lake area, $[km^2]$			
	1	100	1000	
FISH1	0.6	0.4	0	14.0
FISH2	0.6	0.4	0	12.2
FISH3	0.1	0.5	0.4	6.7
FISH4	0.02	0.08	0.9	30.7
FISH5	0.3	0.5	0.2	31.8
FISH6	0.5	0.5	0	15.3

2.5.3 Human intake

The human intake is given as follows:

$$U_{f,HB}(t) = J_f \cdot C_f(t)$$

where

$U_{f,HB}(t)$ is the intake rate of activity of human, [Bq/d]
J_f is the consumption rate of foodstuff, [kg/d]
$C_f(t)$ is the concentration in foodstuff, [Bq/kg].

The typical consumption rates of foodstuffs of the population living in area S, were given in the scenario description [1]. Because of the relatively high deposition values it was felt reasonable to give some recommendations of the consumption rates of some important foodstuffs, such as freshwater fish, by the authorities responsible for radiation safety in area S. Additionally, when predicting the ingestion doses of area S, it was assumed that people will voluntarily reduce temporarily the consumption rates of some foodstuffs. The typical consumption rates and the assumed reduction of consumption rates after deposition are presented in Table XI. The calculation results of area S are based on reduced consumption rates. A reduction of cesium concentrations by decontamination is applied for cereals, vegetables and mushrooms. The decontamination methods generally used for leafy vegetables and mushrooms are washing and boiling. In the case of cereals, the husks can be removed from the grains.

2.5.4 Whole body concentrations

2.5.4.1 Mean whole body concentrations

The prediction of the body burden of human is based on the utilization of the biological half-lives which are known for cesium in the body and on single compartment approximation for the human body. The data used are presented in Table XII. The biological half-lives presented in Table XII are shorter than those proposed by the ICRP. The data for biological half-lives used in this study reflect the studies of whole body contamination measurements performed in Finland [17,18]. The intake rates [Bq/d] described above were used as source-term in the body model. The body masses used for child and female in this study are probably overestimated.

2.5.4.2 Distribution of whole body concentrations (man)

The uncertainty in the input data was studied with the model by performing several computer runs for the considered scenario. At the beginning of each run, a new set of input data was casted from the input data distributions. The cumulative and complementary cumulative probability distribution function (CCDF) was satisfactorily reached after about 30 computer runs. Furthermore, the uncertainty bounds corresponding to 0.95 probabilities were determined for the distributions of the whole body concentrations.

Analyses performed earlier indicated that the uncertainty in predictions for body burdens are contributed mostly by just a few important dose pathways, such as milk. The parameter values of the input data distribution of the milk pathway are presented in Table XIII.

Table XI The consumption rates of foodstuffs [1].

Food-stuff	Type of human	Mean consumption rate, [g/d]	Estimated reduction of consumption rates, [per cent of mean consumption rate]				
			1986	1987	1988	1989	1990
MILK[1]	male	940	30	20	10	0	0
	female	636	30	25	15	5	0
	child (10 yr)	766	20	15	10	0	0
BEEF	male	64	10	0	0	0	0
	female	49	10	0	0	0	0
	child	39	5	0	0	0	0
PORK	male	88	10	0	0	0	0
	female	54	10	0	0	0	0
	child	37	5	0	0	0	0
FISH	male	15	35	25	20	5	0
	female	10	35	25	20	5	0
	child	5	30	20	15	0	0
SMALL GAME							
	male	0.4	25	10	5	0	0
	female	0.3	25	10	5	0	0
	child	0.2	25	10	5	0	0
BIG GAME							
	male	3.8	25	10	5	0	0
	female	3.1	25	10	5	0	0
	child	2.1	25	10	5	0	0
RYE[2]	male	58	0	0	0	0	0
	female	42	0	0	0	0	0
	child	32	0	0	0	0	0
WHEAT[2]							
	male	135	0	0	0	0	0
	female	109	0	0	0	0	0
	child	115	0	0	0	0	0
OAT[2]	male	38	0	0	0	0	0
	female	28	0	0	0	0	0
	child	32	0	0	0	0	0
VEGETABLES[2]							
	male	35	5	0	0	0	0
	female	45	5	0	0	0	0
	child	96	5	0	0	0	0
WILD BERRIES							
	male	9	30	15	0	0	0
	female	9	30	15	0	0	0
	child	9	30	15	0	0	0
MUSHROOMS[2]							
	male	3.6	35	20	10	0	0
	female	3.6	35	20	10	0	0
	child	2.5	35	20	10	0	0

1) Includes the consumption of cheese.
2) Reduction factor by decontamination: 0.1 for cereals and 0.3 for vegetables and mushrooms.

Table XII Data used in the body model.

	Child 10 year	Female	Male
BODY MODEL			
- biological half-life $T_{1/2b}$ for cesium, [d]	50	85	90
- body mass, [kg]	45	65	75

***Table XIII** The input data applied in uncertainty analyses of milk pathway.*

Parameter	μ	min	max
- interception factor	0.3	0.1	0.9
- effective half-life from grass surface, [d]	25	8.3	75
- distribution coefficient in soil, K_d, [liter/kg]	1000	300	10000

2.5.5 Dose calculations

2.5.5.1 External

The prediction approach of external dose from ground is similar to Gale's formula [19]. The mean external dose from contaminated *ground* is given as follows:

$$H_{ext,g}(t)=(\alpha_{t,s}\cdot(f_{MS}\cdot s_{s,MS}+f_{SF}\cdot s_{s,SF})+(1-\alpha_{t,s})\cdot s_{s,out})\cdot d_g\cdot DF\cdot\int(\xi\cdot e^{-(\mu_1+\lambda)\cdot t}+(1-\xi)\cdot e^{-(\mu_2+\lambda)\cdot t})dt$$

where

$H_{ext,g}(t)$	is the individual dose from external exposure from ground, [Sv]
$\alpha_{t,s}$	is the fraction of time spent inside
f_{MS}	is the fraction of population living in multi-storey buildings
f_{SF}	is the fraction of population living in single-family houses
$s_{s,MS}$	is the location factor of multi-storey buildings
$s_{s,SF}$	is the location factor of single-family houses
$s_{s,out}$	is the location factor outside
d_g	is the total deposition on ground, [Bq/m^2]
DF	is the dose conversion factor, [Sv/a]/[Bq/m^2]
ξ	is the fraction of the fast migration component
μ_1	is the removal rate constant of the fast migration, [1/a]
μ_2	is the removal rate constant of the long-term migration, [1/a]
λ	is the radioactive decay rate, [1/a].

The mean external dose from *plume* is given as follows:

$$H_{ext,c}(t)=\frac{\zeta_{POP8}+\zeta_{OTHER}\cdot 0.02^{*}}{\zeta_{ALL}}\cdot(\alpha_{t,s}\cdot(f_{MS}\cdot s_{s,MS}+f_{SF}\cdot s_{s,SF})+(1-\alpha_{t,s})\cdot s_{s,out})\cdot g_{Y}\cdot\int C_{a,POP8}(t)dt$$

where

$H_{ext,c}(t)$	is the dose from external exposure from plume, [Sv]
g_Y	is the external dose conversion factor, [Sv/h]/[Bq/m^3]
ζ_{POP8}	is the population of sub-area POP8
ζ_{OTHER}	is the total population of other sub-areas than POP8
ζ_{ALL}	is the population of the whole area S
$C_{a,POP8}(t)$	is the cesium concentration in air of POP8, [Bq/m^3].

* Measurements of total activity in air from ten stations of another monitoring network showed significantly lower concentrations outside the subarea POP8 and the southern half of POP7 than at stations AIR1 and AIR2. During 27.4.–1.5.1986, the total activities in air at stations in the subareas *did not exceed 2%* of those measured at AIR2 [1].

The data for external dose calculations are presented in Table XIV.

Table XIV Data used in the external dose models.

	Reference	General data of the model	Data for ^{137}Cs nuclide
EXTERNAL DOSE FROM GROUND			
- fraction of time spent inside		0.95	
- fraction of population living in multi-storey buildings		0.5	
- fraction of population living in single-family houses		0.5	
- location factor$^{1)}$ of multi-storey buildings	[21]		0.05
- location factor of single-family houses	[21]		0.5
- dose conversion factor$^{2)}$, [Sv/a]/[Bq/m^2]	[1]		$1.1 \cdot 10^{-8}$
- fraction of the fast migration component	[20]		0.63
- removal rate constant of the fast migration, [1/a]	[20]		1.13
- removal rate constant of the long-term migration, [1/a]	[20]		0.0075
EXTERNAL DOSE FROM PLUME			
- dose conversion factor, [Sv/a]/[Bq/m^3]	[1]		$8.1 \cdot 10^{-7}$
- shielding factor of multi-storey buildings	[21]		0.2
- shielding factor of single-family houses	[21]		0.5

1) Location factor accounts for the modification of the reference dose rate at different locations [21].

2) Includes shielding caused by roughness of terrain.

The variation of location factors is large, depending on the types of buildings and also on the living habits of the population exposed to external radiation. Recent research work [21] concerning location factors in the Nordic countries proposes the following variation of location factors applicable for Finland for external exposure from ground: 0.01–0.05 for multi-storey buildings, 0.04–1 for single-family houses. The proposed shielding factors in the case of external exposure from plume are: 0.016–0.33 for multi-storey buildings, 0.27–0.52 for single-family houses. The recent studies, carried out in Finland, support also the values of location and shielding factors presented above.

2.5.5.2 Ingestion

The individual ingestion dose is given as:

$$H_{ing,HB}(t)=d_i \cdot J_f \cdot \int C_f(t)dt$$

where

$H_{ing,HB}(t)$	is the individual ingestion dose, [Sv]
$C_f(t)$	is the concentration in a foodstuff, [Bq/kg]
J_f	is the consumption rate of a foodstuff, [kg/a]
d_i	is the ingestion dose conversion factor, [Sv/Bq].

The total ingestion dose will be obtained by summing up the dose contributions from all the considered foodstuffs. The consumption rates of foodstuffs and ingestion dose conversion factor ($1.4 \cdot 10^{-8}$ Sv/Bq) of ^{137}Cs were given in the scenario description [1]. However, as discussed earlier in chapter 2.5.3, the consumption rates of some foodstuffs by humans were reduced to some extent during the first two to three years after deposition.

2.5.5.3 Inhalation

The mean inhalation dose arising from *resuspended material* in air is given as follows:

$$H_{a,r}(t)=\alpha_{t,out} \cdot J_I \cdot \vartheta \cdot d_I \cdot \int C_s(t)dt$$

where

$H_{a,r}(t)$	is the mean inhalation dose from resuspension to individual, [Sv]
$\alpha_{t,out}$	is the fraction of time spent outside
J_I	is the inhalation rate, [m_a^3/h]
ϑ	is the soil concentration in air, [kg/m_a^3]
d_I	is the inhalation dose conversion factor, [Sv/Bq]
$C_s(t)$	is the activity concentration in soil, [Bq/kg].

The temporal behaviour of the activity concentration of cesium in soil $C_s(t)$ is predicted based on the compartment model approach as presented in Fig. 5 above. Taking into account the soil concentration in air ϑ (see Table XV) and the calculated activity concentration in soil, the initial resuspension factor was derived to be about $7 \cdot 10^{-8}$ 1/m. This resuspension value is relevant looking at the observed resuspension values for the Nordic environment as presented in ref. [14]. In the longterm, the decrease of the resuspension factor is proportional to the decrease of activity concentration in the top soil layer.

The mean inhalation dose arising from the original radioactive *plume* is given as follows:

$$H_{a,c}(t) = \frac{\zeta_{POP8} + \zeta_{OTHER} \cdot 0.02^{*}}{\zeta_{ALL}} \cdot d_I \cdot J_I \cdot \int C_{a,POP8}(t)dt$$

where

$H_{a,c}(t)$	is the mean inhalation dose from plume to individual, [Sv]
ζ_{POP8}	is the population of sub-area 8
ζ_{OTHER}	is the total population of other sub-areas than 8
ζ_{ALL}	is the population of the whole area S
d_I	is the inhalation dose conversion factor, [Sv/Bq]
J_I	is the inhalation rate, [m^3/h]
$C_{a,POP8}(t)$	is the cesium concentration in the air of POP8, [Bq/m^3].
*	See explanation on previous page 21.

The data used in prediction of inhalation doses are presented in Table XV.

Table XV *Data used in the inhalation model.*

	Reference	General data of the model	Data for ^{137}Cs nuclide
INHALATION			
- fraction of time spent outside[1]		0.1	
- inhalation rate[1], [m^3/h]		0.8	
- soil content in air[1),2)], [kg/m^3]			$1 \cdot 10^{-6}$
- inhalation dose conversion factor, [Sv/Bq]	[1]		$8.6 \cdot 10^{-9}$

1) See explanation 3) under Table I.
2) The activity concentration of resuspended material in air is calculated from a homogenized soil layer up to 0.5 cm from the soil surface.

2.6 Identification of important processes and parameters

For the terrestrial pathways, the weathering effects on the surface of e.g. grass affect significantly the cesium activity contents of several foodstuffs. The migration rate of cesium in surface soil affects also long-term concentrations in wild berries, mushrooms and game. According to measurements, the cesium concentration in forest soil has reduced slowly. The calculations performed support the observed behaviour.

Looking at the aquatic environment, the dilution properties of various lakes affect the concentration of lake water as well as the concentrations in fish. The strong dynamic behaviour of the trophic chain of different fish types causes a long lasting contamination effect in the aquatic environment after deposition.

3 COMPARISON OF OBSERVED DATA AND MODEL PREDICTIONS

3.1 Total deposition

The predicted mean total deposition 19.3 kBq/m^2 over the whole area S was consistent with the observed value. Correspondingly, the predicted total inventory $3.4 \cdot 10^{15}$ Bq, calculated from the deposition value, was almost identical with the given inventory value $3.5 \cdot 10^{15}$ Bq [1].

3.2 Foodstuffs contributing to total diet

3.2.1 Milk

The observed values of Scenario S of the VAMP research programme were prepared for IAEA by the Finnish Centre for Radiation and Nuclear Safety and they are presented in publication [1]. Fig. 8 presents the temporal behaviour of observed and predicted concentrations of ^{137}Cs in milk. For the first year after the deposition, the model predicts well the activity content in milk. Thereafter, the uncertainty bounds of the predicted values cover the observed values although there is a tendency of underestimation of the concentration level in the longterm.

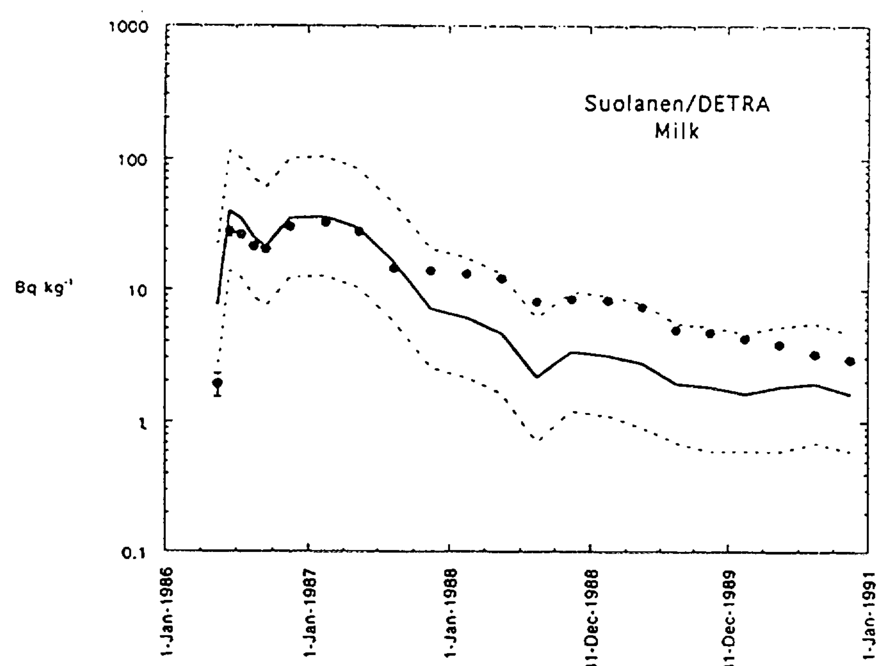

● = observed value [1]
--- = predicted 95 % confidence interval (lower bound and upper bound)
— = predicted mean value

Fig. 8. Observed and predicted concentrations of ^{137}Cs in milk.

3.2.2 Beef

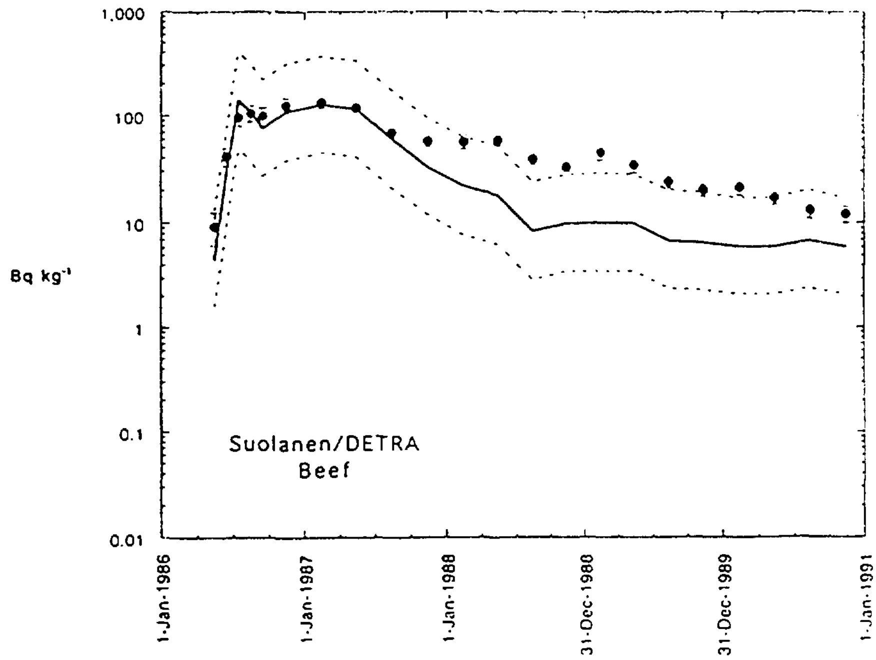

Fig. 9. Observed and predicted concentrations of ^{137}Cs in beef.

3.2.3 Pork

Considering the long-term concentrations in pork, the model clearly underestimates the contamination level. The reasons for underestimation will be discussed later in chapter 4.2.

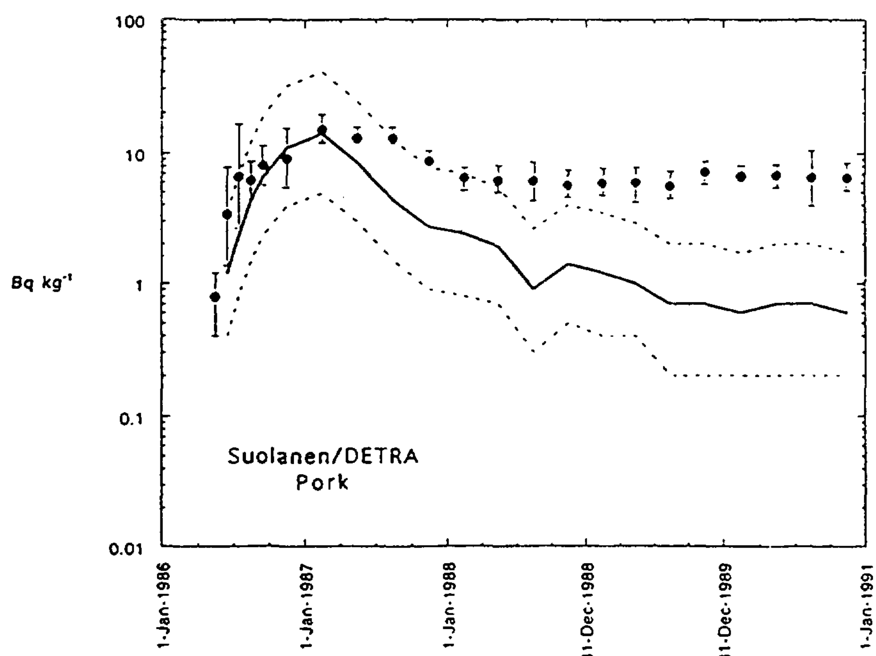

Fig. 10. Observed and predicted concentrations of ^{137}Cs in pork.

3.2.4 Game

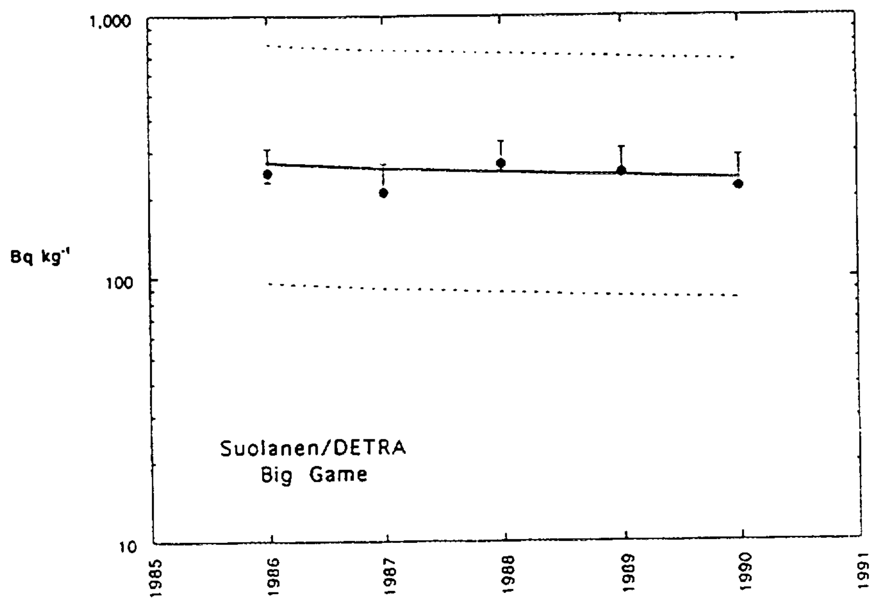

Fig. 11. *Observed and predicted concentrations of ^{137}Cs in big game.*

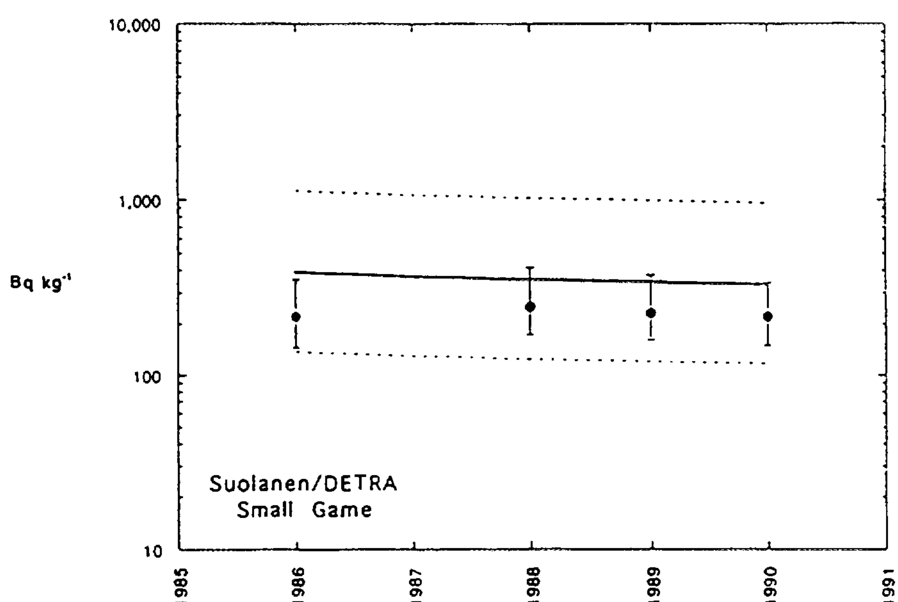

Fig. 12. *Observed and predicted concentrations of ^{137}Cs in small game.*

3.2.5 Wild berries

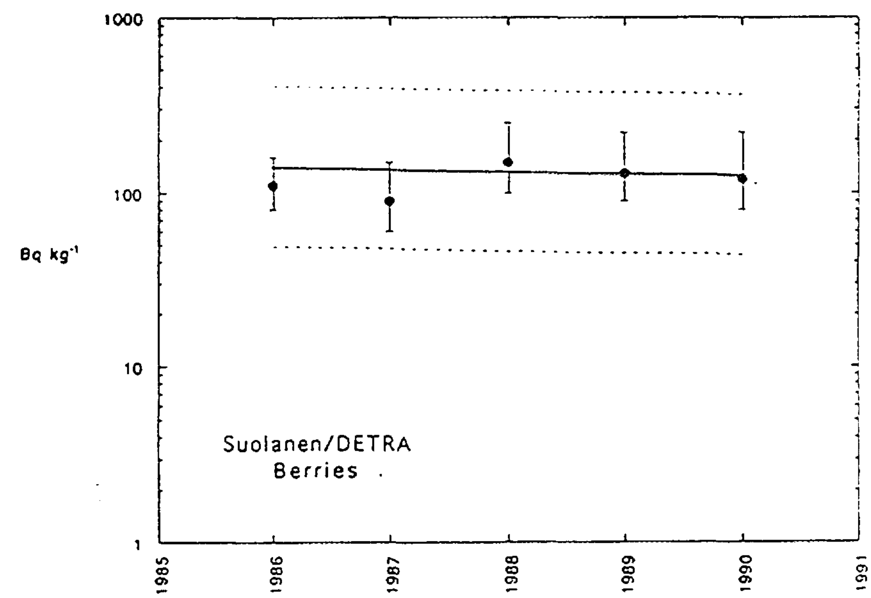

Fig. 13. Observed and predicted concentrations of ^{137}Cs in wild berries.

3.2.6 Mushrooms

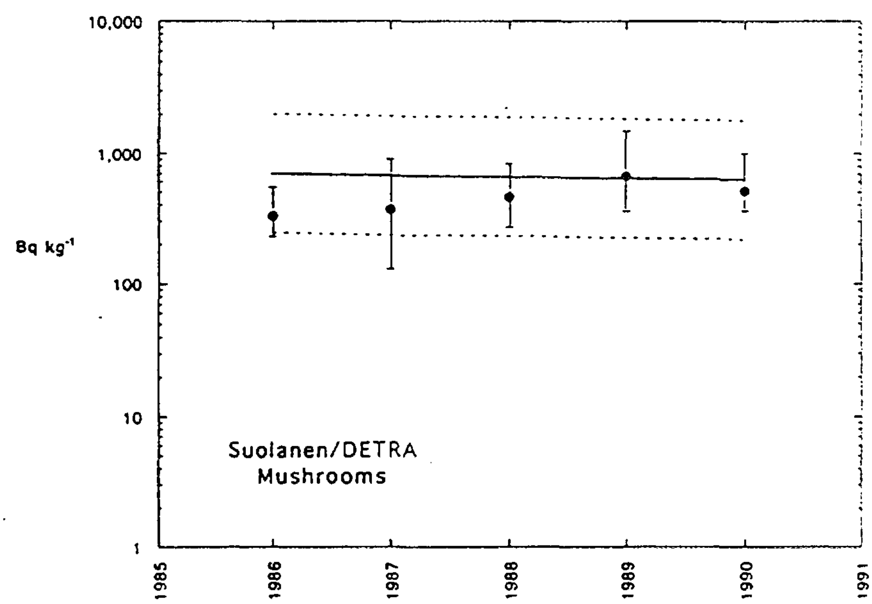

Fig. 14. Observed and predicted concentrations of ^{137}Cs in mushrooms.

3.2.7 Leafy vegetables

Fig. 15. presents the observed vs predicted concentrations of ^{137}Cs in leafy vegetables. The deposition from the Chernobyl nuclear accident is unevenly distributed over the area of Test Scenario S. The intensity of greenhouses in area S is also unevenly distributed. Additionally, deposition in area S was mainly of the wet type. The facts mentioned above affect the accuracy of predictions especially in the case of vegetables produced in the greenhouses.

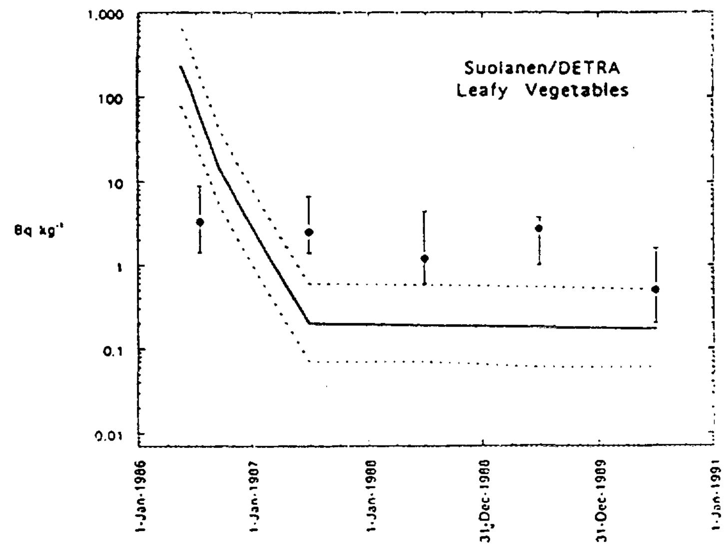

Fig. 15. Observed and predicted concentrations of ^{137}Cs in leafy vegetables.

3.2.8 Cereals

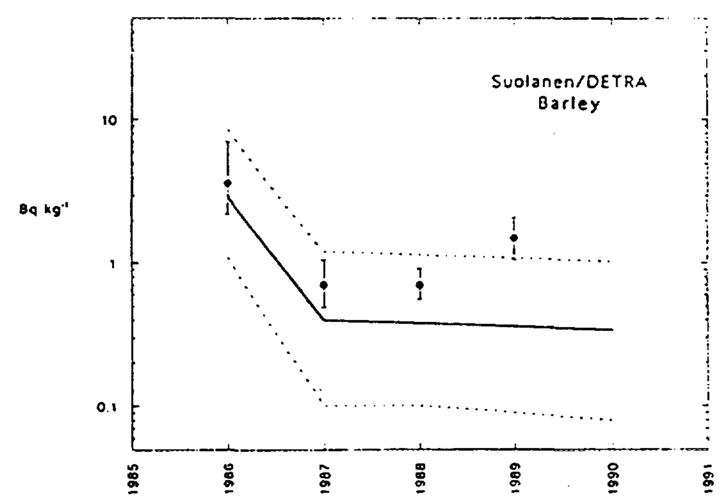

Fig. 16. Observed and predicted concentrations of ^{137}Cs in barley.

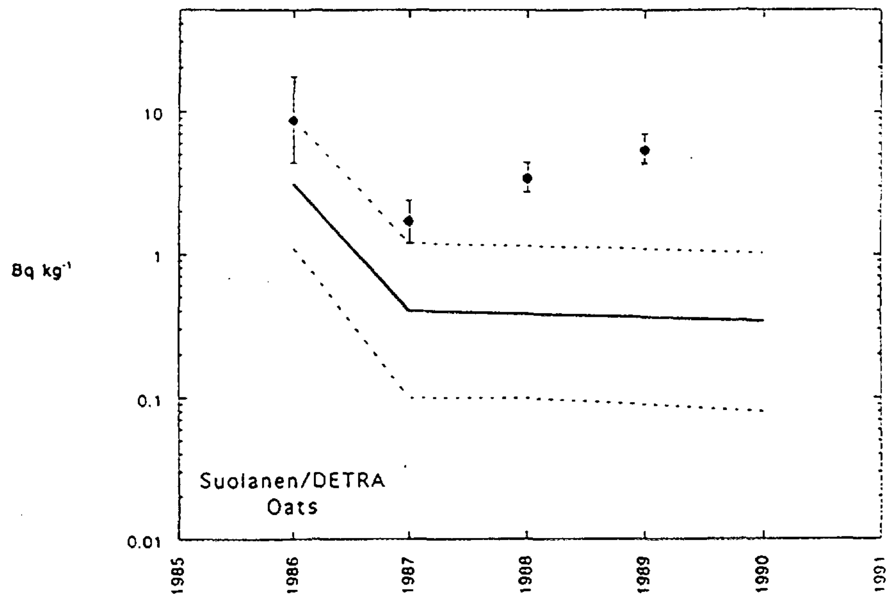

Fig. 17. *Observed and predicted concentrations of ^{137}Cs in oats.*

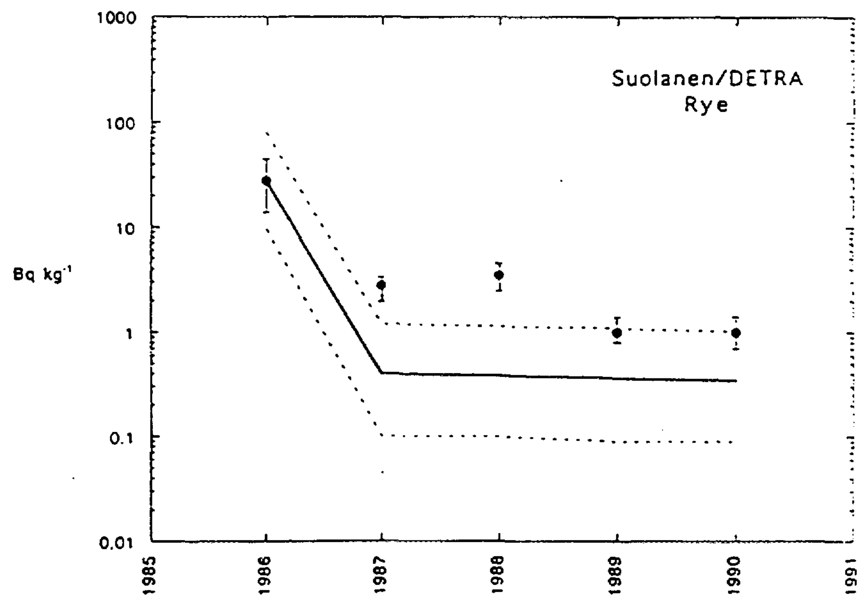

Fig. 18. *Observed and predicted concentrations of ^{137}Cs in rye.*

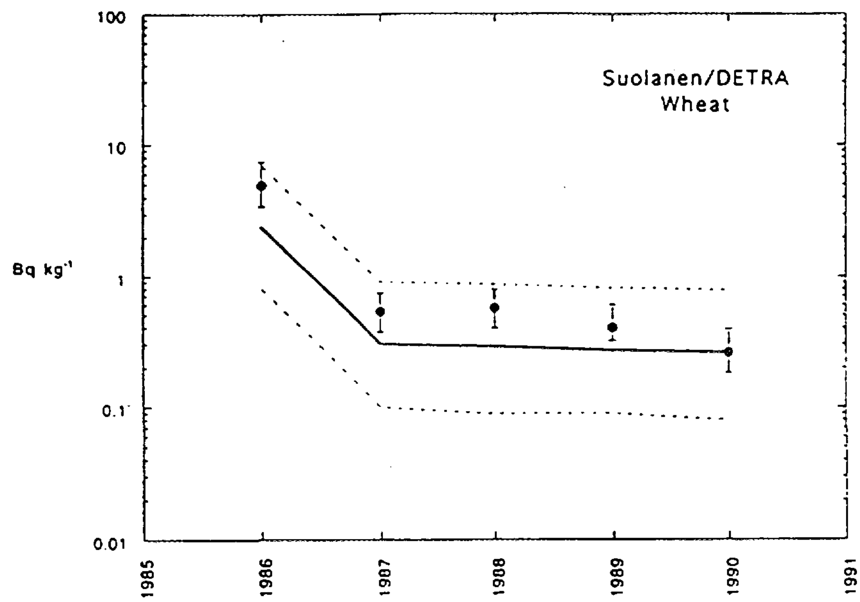

Fig. 19. *Observed and predicted concentrations of ^{137}Cs in wheat.*

3.2.9 Fish

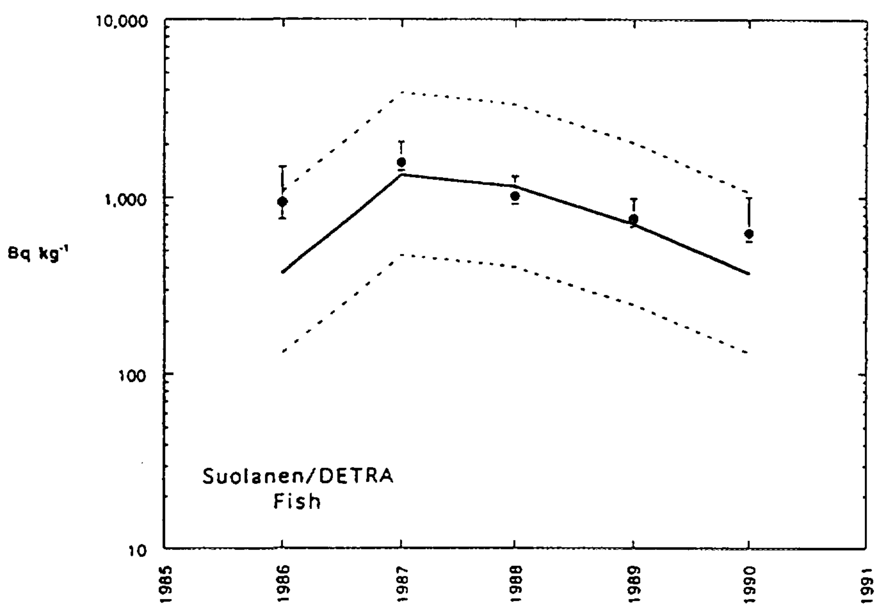

Fig. 20. *Observed and predicted concentrations of ^{137}Cs in fish.*

3.3 Human intake

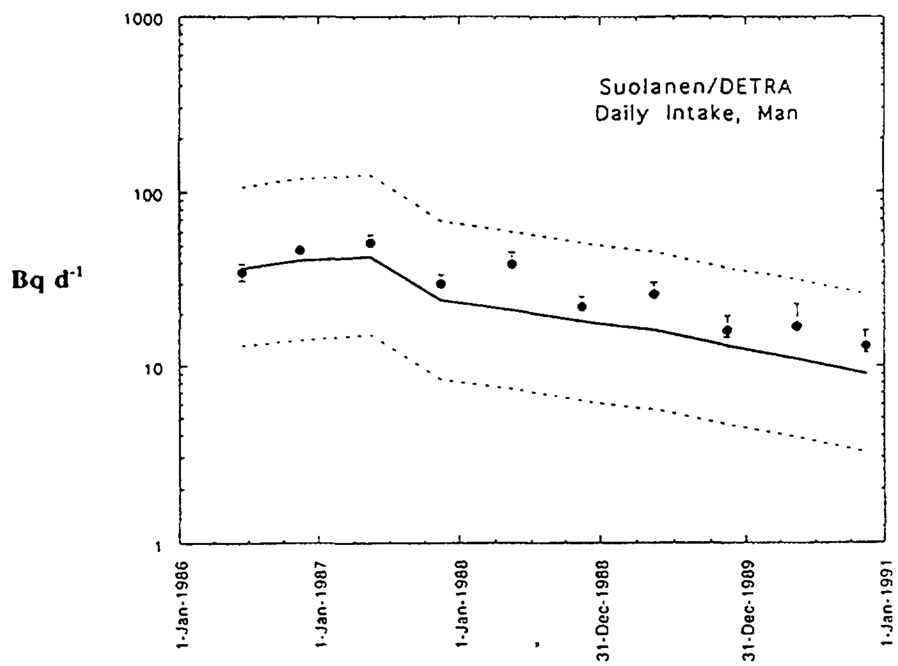

Fig. 21. *Daily intake of ^{137}Cs, man.*

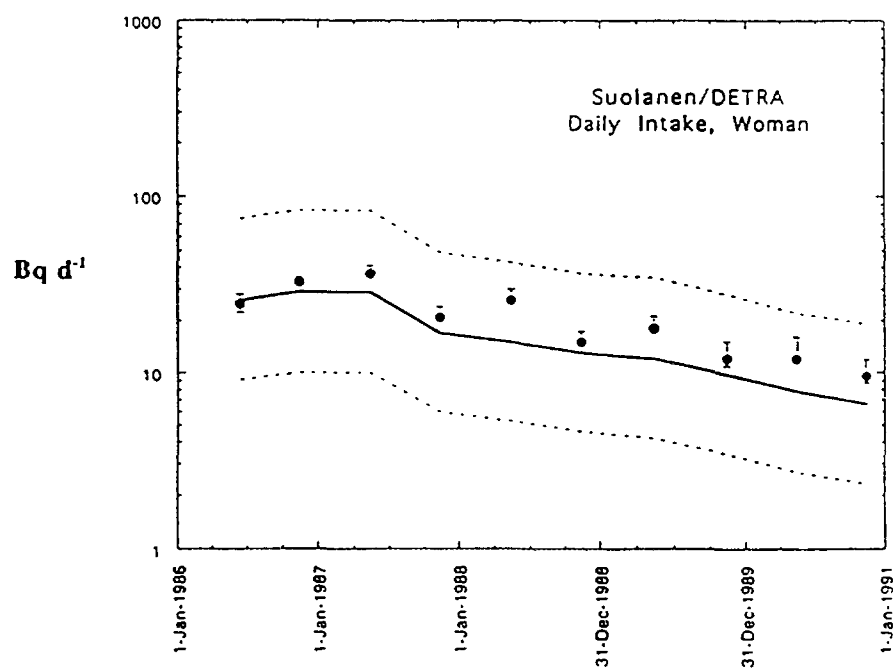

Fig. 22. *Daily intake of ^{137}Cs, woman.*

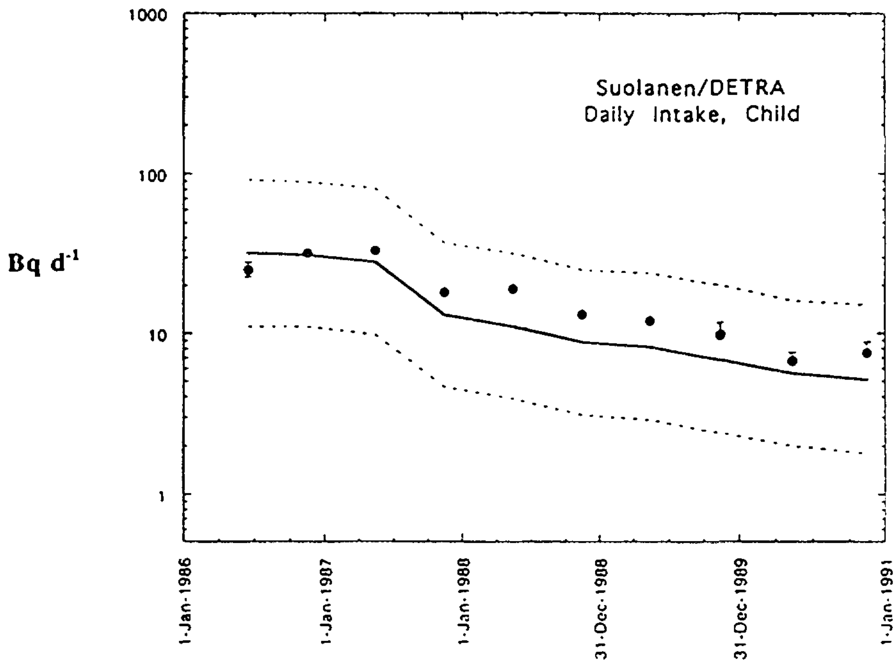

Fig. 23. *Daily intake of ^{137}Cs, child.*

3.4 Whole body concentrations

3.4.1 Mean whole body concentration

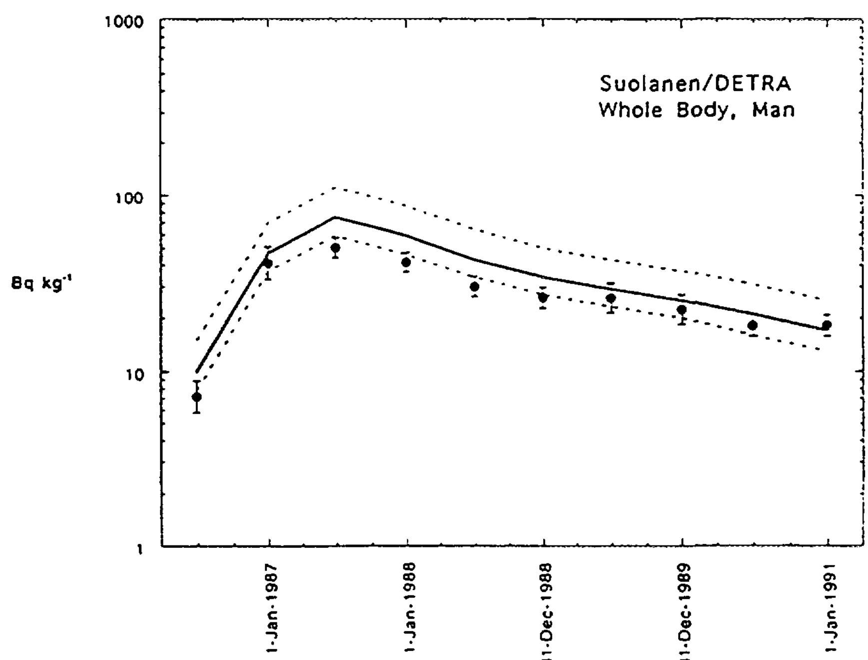

Fig. 24. *Whole body concentration of ^{137}Cs, man.*

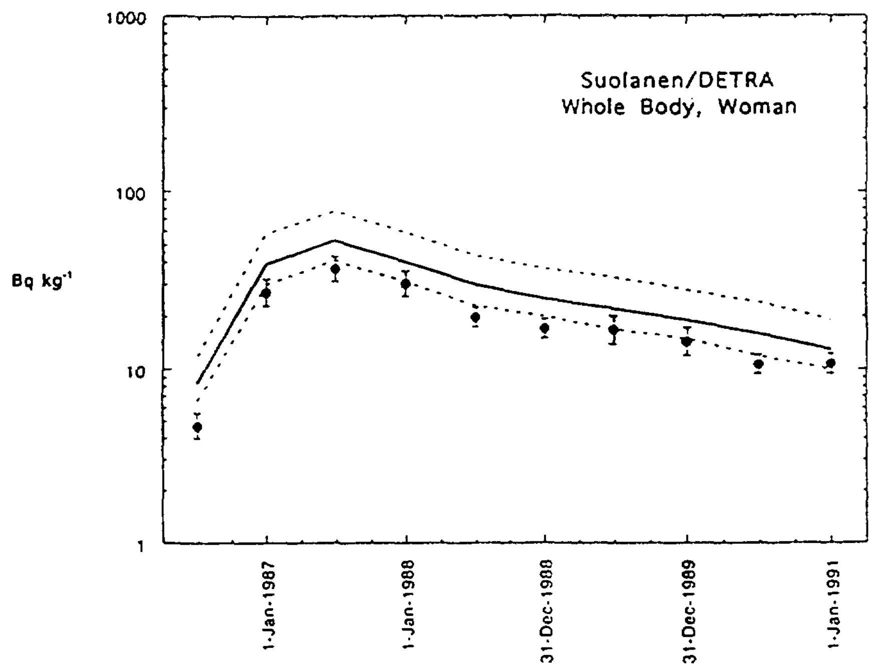

Fig. 25. *Whole body concentration of ^{137}Cs, woman.*

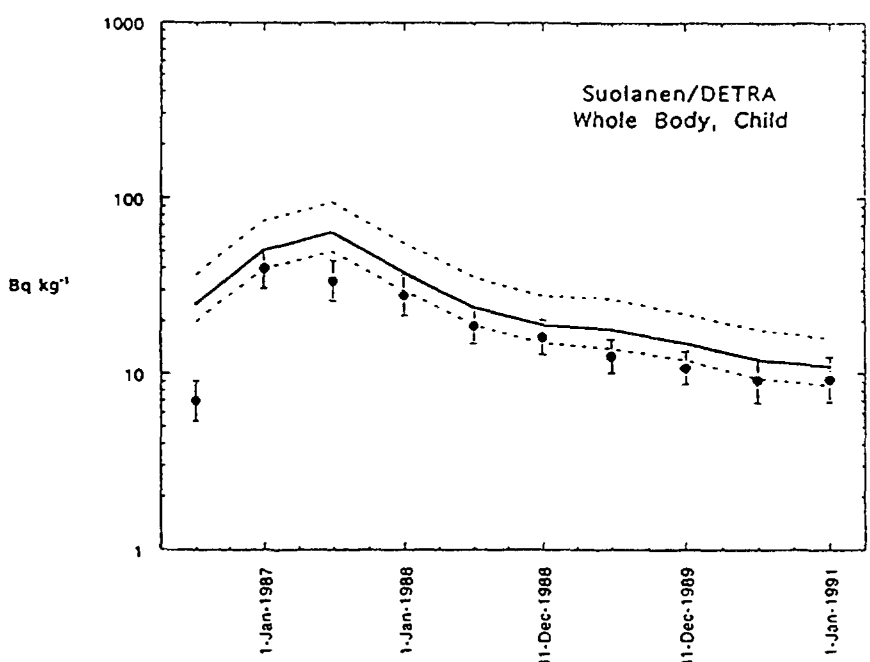

Fig. 26. *Whole body concentration of ^{137}Cs, child.*

3.4.2 Distribution of whole body concentrations

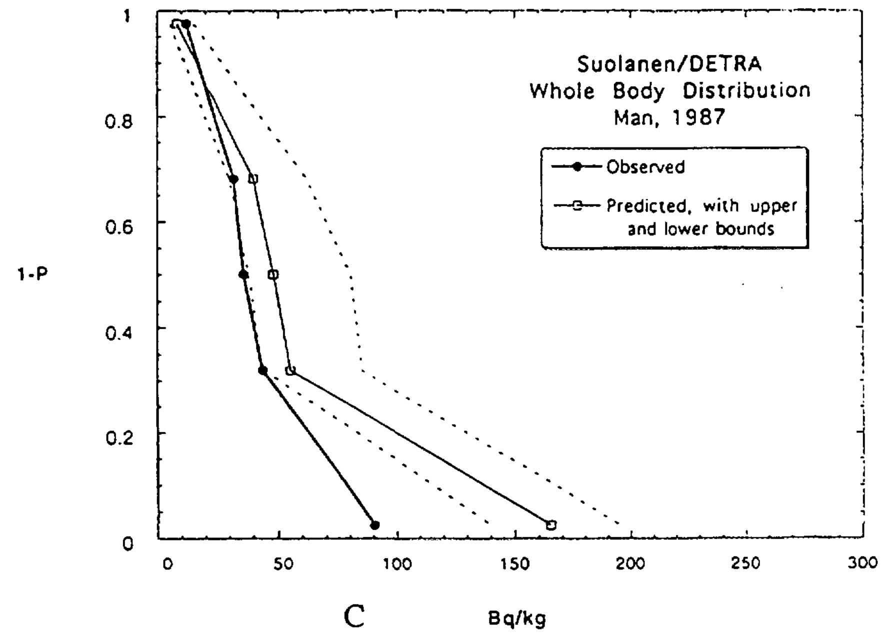

1-P = P(conc. ≥ C)

Fig. 27. *Whole body distribution of concentration of ^{137}Cs, man, 1987.*

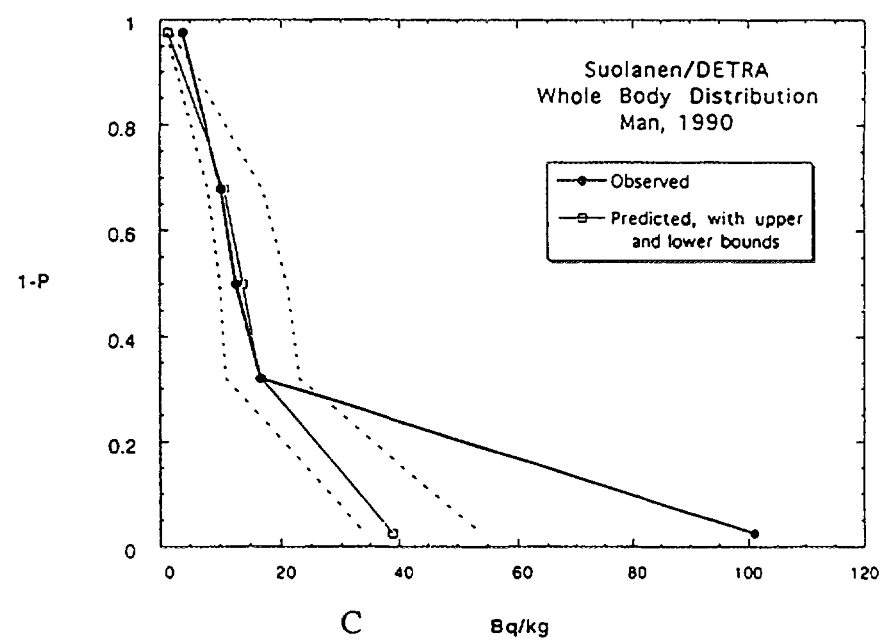

1-P = P(conc. ≥ C)

Fig. 28. *Whole body distribution of concentration of ^{137}Cs, man, 1990.*

3.5 Dose calculations

3.5.1 External

Fig. 29 presents the estimated values [1] and predicted values for a lifetime external dose of ground exposure based on different models. External dose from plume exposure is presented in Fig. 30.

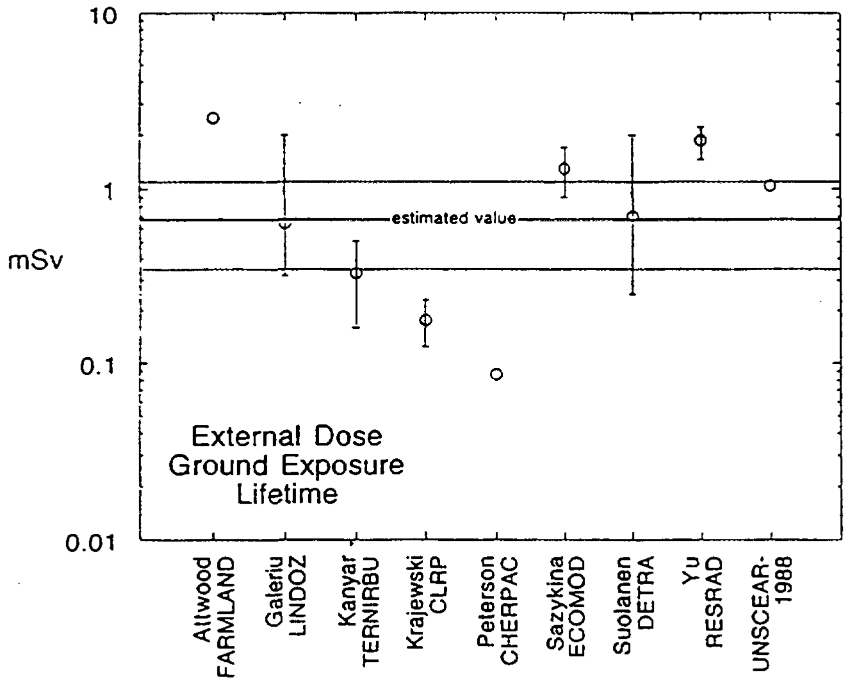

Fig. 29. External dose of ^{137}Cs from ground exposure, estimated and predicted values.

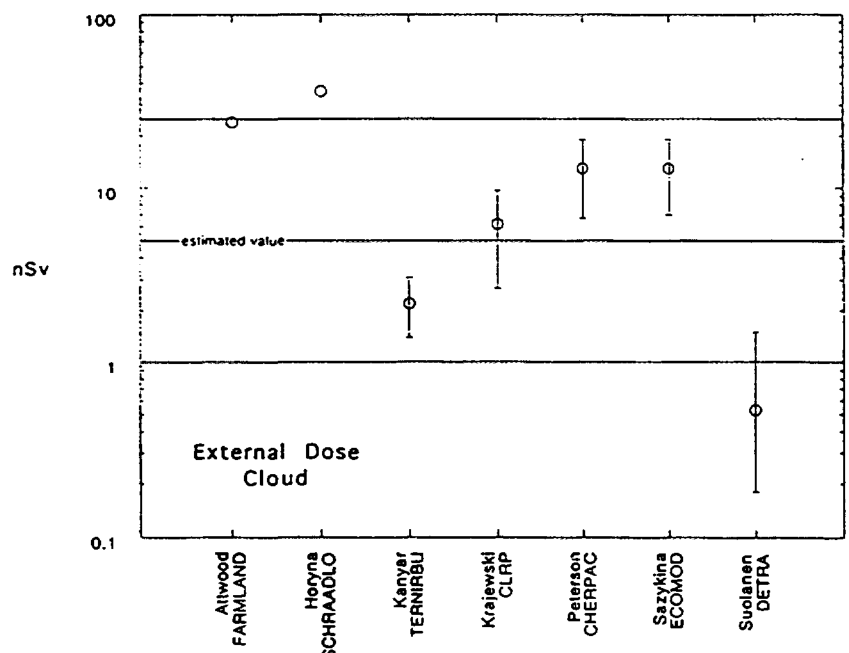

Fig. 30. External dose of ^{137}Cs from plume exposure, estimated and predicted values.

3.5.2 Ingestion

Fig. 31 presents the estimated [1] and predicted lifetime doses from ingestion of contaminated foodstuffs. All models conclude that freshwater fish has the highest contribution to ingestion dose of Scenario S in the long-term consideration.

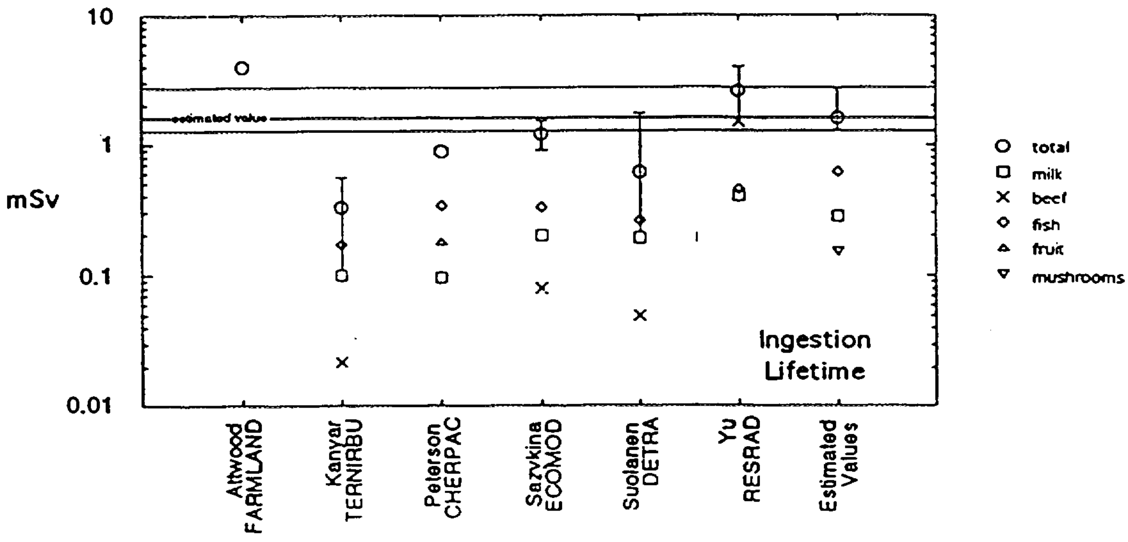

Fig. 31. *Ingestion lifetime doses of ^{137}Cs.*

3.5.3 Inhalation

Inhalation makes a minor contribution to the total dose arising from the deposition of Scenario S. Figures 32 and 33 present the predicted inhalation doses from resuspension and from plume.

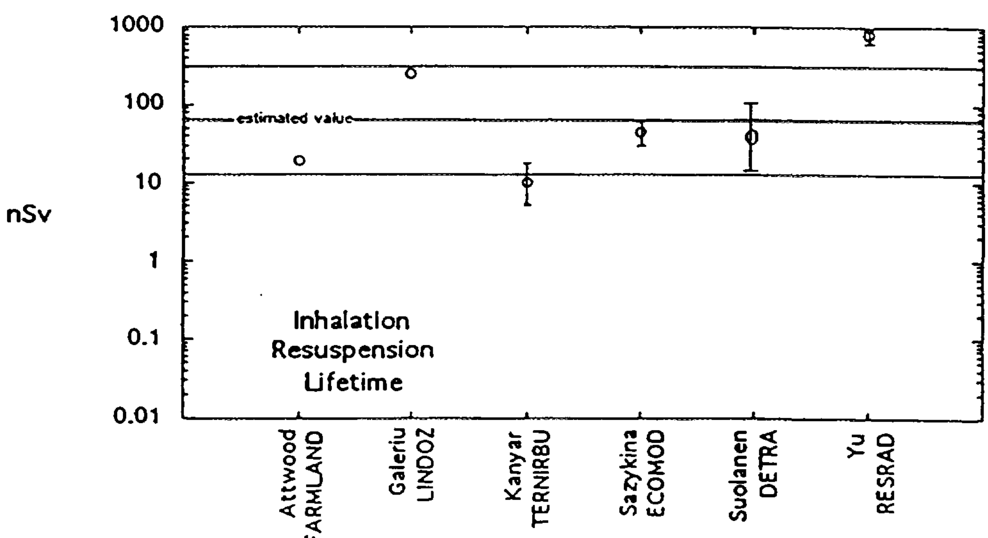

Fig. 32. *Inhalation lifetime doses of ^{137}Cs from resuspension.*

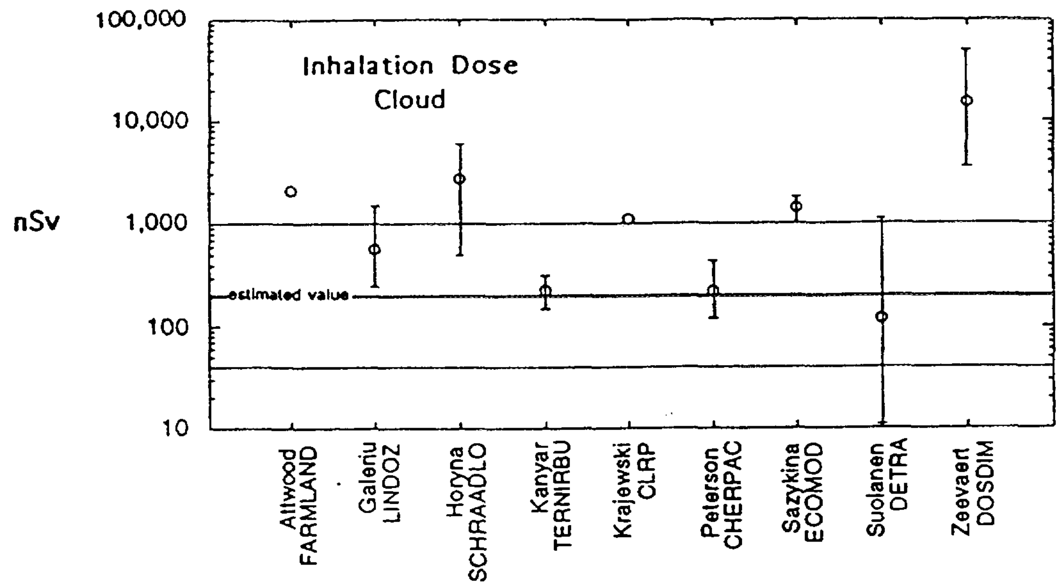

Fig. 33. *Inhalation dose of ^{137}Cs from plume.*

Total doses, predicted by various models, are presented in Fig. 34[1].

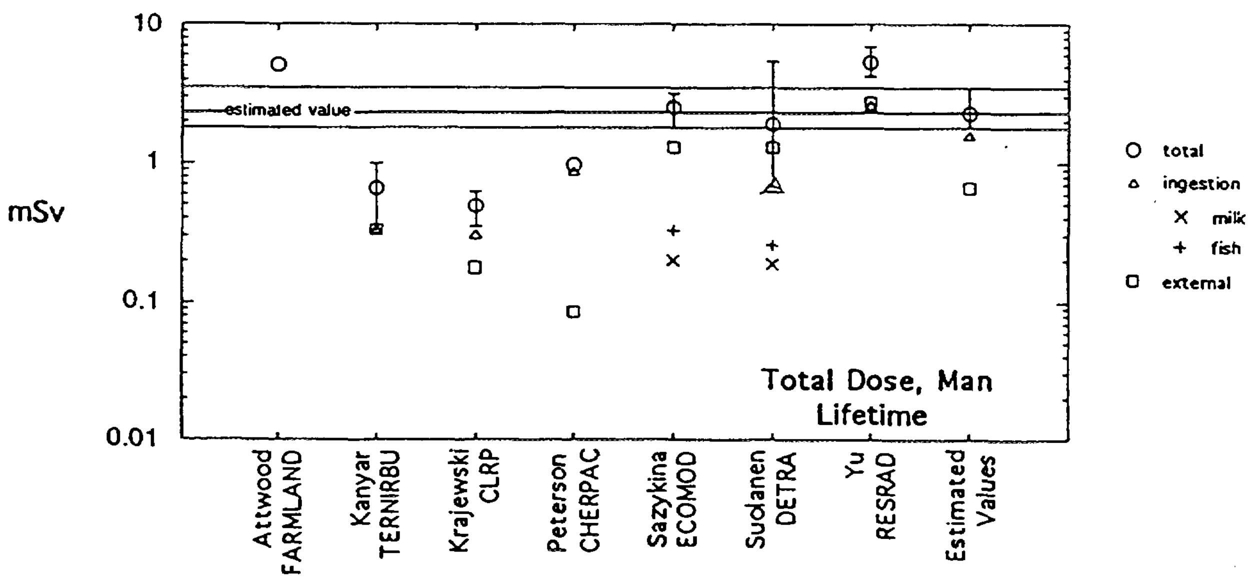

Fig. 34[1]. *Total lifetime doses of ^{137}Cs over the entire region S.*

1) The results of DETRA presented in the figure are based on a preliminary analysis which employed more conservative values for the location and the shielding factors than those presented in Table XIV above. In the final published version of this report the figure will be replaced accordingly.

4 EXPLANATION OF MAJOR SOURCES OF MISPREDICTION

4.1 Recommendations for changes to the model

Effects of uncertainty factors on the predictions of Scenario S seemed to occur in the long-term considerations. Possible reasons for this include heterogeneity related to the agricultural practices of different farms, such as the production of feeds, and changes in the solubility of radionuclides in the longterm. The conceptual models applied as the bases of calculations simplify and homogenize the real agricultural practices to some extent.

To improve the model, more detailed analyses of the importance of various phenomena in different dose pathways should be carried out. As a result, the main activity flows related to contamination of foodstuffs could possibly be clarified even better than it is known at present.

4.2 Examples of how changes improved calculation

The model used to predict the contamination of pork underestimated the long-term cesium concentrations in pork. After careful investigation of the reasons for such underestimation it seemed evident that the reason might be the underestimation of the concentration in mixed grain. In the case of Scenario S, the activity content of cereals started to increase some years after the deposition. If this increase in the activity content of mixed grain is accounted for, a more consistent behaviour with the observed values can be obtained, as illustrated in Fig. 35. In the longterm, some of the difference between the observed and predicted values for concentration in pork is probably caused by an underestimation of the consumption rate of cereal feed for pigs.

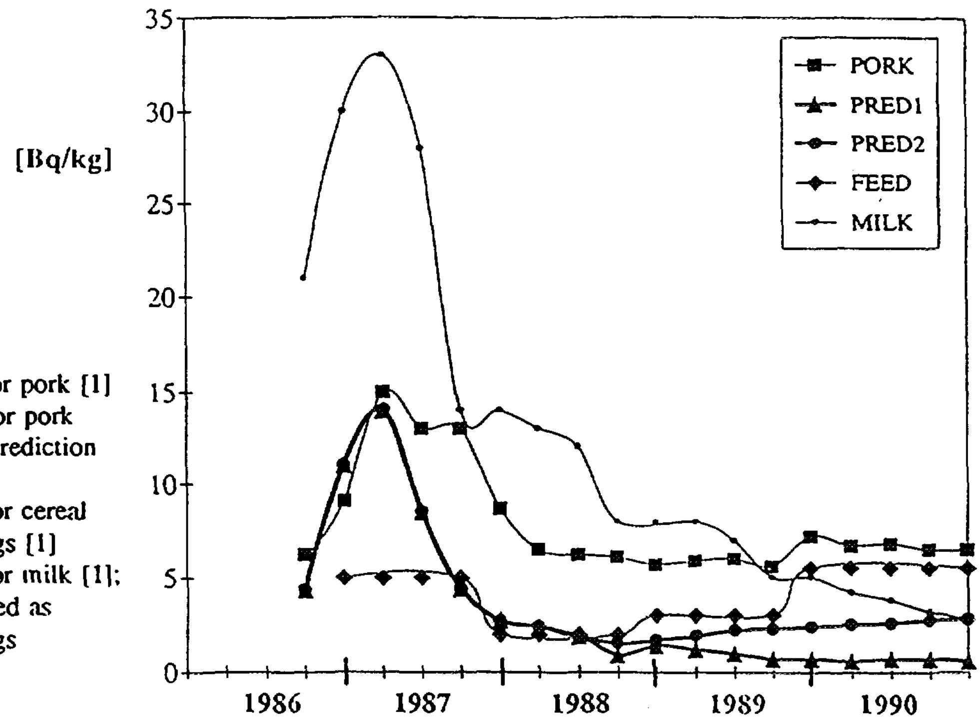

PORK = observed for pork [1]
PRED1 = predicted for pork
PRED2 = improved prediction for pork
FEED = observed for cereal feed for pigs [1]
MILK = observed for milk [1]; whey is used as feed for pigs

Fig. 35. Example of the effect of model development on the pork pathway.

5 SUMMARY OF LESSONS LEARNED FROM THE SCENARIO

Based on the experiences of predictions performed for Scenario S, successful modelling of milk pathway is essential considering the exposure from terrestrical pathways. Activity concentration in milk byproduct, whey, also affect the activity concentration in pork, and the model of milk pathway is also closely related to the model of beef. The modelling of activity contents in soil and pasture also has similarities compared to modelling the activity content in the forest environment.

Looking at the aquatic environment, freshwater fish have proved important and, according to the analyses performed, it was the most important foodstuff considering the total individual ingestion dose in the longterm.

According to the observations, the ingestion dose contributes most to the estimated total life-time dose for the population living in the area of Scenario S.

The parameters applied in the models of this study are in most cases relevant, especially considering the features of the Finnish environment. The parameters of some pathways are derived based on the practices in national agriculture. In case a deposition should occur in the northern part of Finland, there are some important arctic dose pathways which were not included in this study because the deposition of the Chernobyl accident and the area of Scenario S concerned only the southern and middle parts of Finland.

The models and off-site parameters employed in this study are also in most cases applicable to unexpected severe accidents in either of the Finnish nuclear power plants, the Olkiluoto NPP or the Loviisa NPP. Factors which will essentially change the input data applied in this study include seasonality, production data of foodstuffs and dilution properties of inland freshwater recipients. Seasonality directly affects the interception of grass and other vegetation. Production rates of domestic animal products, feeds and dilution factors of lakes affect the level of concentrations obtained in foodstuffs after a deposition. In any case, rough dose estimates, as derived from the results of this study are applicable in case a radioactive deposition should happen at some other time of the year than in the case of Test Scenario S.

REFERENCES

[1] Rantavaara, A., Scenario description and observed values for test area S, Co-ordinated Research Programme on Validation of Environmental Model Predictions (VAMP), Multiple Pathways Assessment (MPA), IAEA, to be published in 1994.

[2] Validation of Environmental Model Predictions (VAMP). A programme for testing and improving biospheric models using data from the Chernobyl fallout. Background to the programme and progress to date. IAEA, 1993.

[3] Korhonen, R., Savolainen, I., Biospheric transfer model DETRA for assessment of radiation impacts. Technical Research Centre of Finland, Nuclear Engineering Laboratory, Research Reports 323, Espoo 1984 (in Finnish).

[4] Korhonen, R., Model studies of the transfer of radionuclides in the Finnish environment. Technical Research Centre of Finland, Nuclear Engineering Laboratory, Publications 81 (Thesis), Espoo 1991.

[5] Kliment, V., Contamination of pork by caesium radioisotopes. Institute of Hygiene and Epidemiology - Centre of Radiation Hygiene, Czechoslovakia, 1990.

[6] Müller, H., Pröhl, G., Cesium transport in food chains – comparison of model predictions and observations. Proceedings of CEC Workshop on "Methods for Assessing the Reliability of Environmental Transfer Models Predictions", Athens, October 5-9, 1987. Reliability of Radioactive Transfer Models (editor G. Desmet), Elsevier Applied Science, London 1988, pp. 104-113.

[7] Maubert, H., Roussel, S., Dynamic model of food chain transfer subsequent to radioactive fallout. OECD/NEA&CEC Workshop on Recent Advances in Reactor Accident Consequence Assessment, Rome, 25-29 January, 1988.

[8] Kakko, R., Partanen, J., Estimated doses via ingestion of contaminated foodstuffs after radioactive deposition. Technical Research Centre of Finland (VTT), Research Notes 292, Espoo 1984 (in Finnish).

[9] Linsley, G.S., Simmonds, J.R., Kelly, G.N., An evaluation of the food chain pathway for transuranium elements dispersed in soils. Harwell 1978. National Radiological Protection Board, NRPB-R-81.

[10] Frissel, M.J., Koster, J., The IUR project on soil-to-plant transfer factors of radionuclides – expected values and uncertainties. Proceedings of CEC Workshop on "Methods for Assessing the Reliability of Environmental Transfer Models Predictions", Athens, October 5-9, 1987. Reliability of Radioactive Transfer Models (editor G. Desmet), Elsevier Applied Science, London 1988, pp. 151-158.

[11] Watkins BM. Interception, retention, absorption and translocation of radionuclides by vegetation following application in irrigation waters. NSS/R221, 1990.

[12] Handbook of parameter values for the prediction of radionuclide transfer in temperate environments (draft), IAEA, 1993.

[13] The Palmottu Analogue Project, Progress Report 1992 (edited by: L. Ahonen, R. Blomqvist, and J. Suksi). Geological Survey of Finland, Nuclear Waste Disposal Research, Report YST-82, Espoo 1993.

[14] Environmental consequences of releases from nuclear accidents, a Nordic perspective. Final report of the NKA project AKTU-200. Edited by U. Tveten, Institute for Energy Technology, Kjeller, Norway, 1990.

[15] Stara JF, Nelson NS, Della Rosa RJ, Bustard LK. Comparative metabolism of radionuclides in mammals. Health Physics 20, 1971.

[16] Nair, S., Iijima, T., Final Report on International Foodchain Data Comparison Exercise "Deposition on Crops and Root Uptake", NEA/OECD Document SINDOC(83) 158 March 1984.